Age of Loop for Wireless Networked Control System in the Finite Blocklength Regime: Average, Variance and Outage Probability

Jie Cao, *Graduate Student Member, IEEE,* Xu Zhu, *Senior Member, IEEE,* Sumei Sun, *Fellow, IEEE,* Petar Popovski, *Fellow, IEEE,* Shaohan Feng, *Member, IEEE,* and Yufei Jiang, *Member, IEEE*

Abstract

Age of information (AoI) is an effective measure of the information freshness for wireless networked control systems (WNCSs). However, the AoI performance for a closed loop of WNCS with two-way delays has remained unexplored, especially in the finite blocklength (FBL) regime. In this paper, we investigate the peak age of loop (PAoL) performances, including the average, variance and outage probability of PAoL, for WNCSs with FBL over fading channels. Their closed-form expressions are respectively derived regarding the blocklength and maximum number of allowable transmissions. We prove that the average PAoL is less than the sum of the average peak AoI in uplink (UL) and downlink (DL) due to the coupling between UL and DL. Also, the relationship between the three PAoL performance metrics is analyzed. It is shown that there is a tradeoff between the average PAoL and the variance/outage probability of PAoL. Based on the comprehensive performance analysis, a PAoL-oriented communication and control co-design is conducted with an effective blocklength adaptation scheme. Simulation results verify the correctness of the analytical results and show that the proposed PAoL-oriented scheme significantly outperforms the UL only and DL only optimization schemes, with an up to 8-fold reduction in the average control cost.

Index Terms

Age of information, finite blocklength, communication and control co-design

Part of this work has been accepted for presentation at IEEE INFOCOM AoI Workshop 2022 [1].

I. INTRODUCTION

Timely information access is required in real-time applications such as factory automation and power system control [2], where the outdated packets with stale information may lead to erroneous operations [3]. To measure information freshness, age of information (AoI) was proposed and defined as the time elapsed since the generation of the latest successfully received status update [3]. Peak AoI (PAoI) captures the worst case of AoI and is much more tractable [4], [5], and hence is analyzed in this paper.

Wireless networked control system (WNCS) is applied in various emerging real-time applications, thanks to its enhanced flexibility and the reduced deployment costs [6]. In WNCSs, each sensor/controller transmits the state/action to a controller/actuator over wireless networks to achieve a control objective [6]. Thus, it is important to characterize the information freshness of WNCSs with two-way delays in order to ensure timely transmission and accurate control in WNCSs.

In a real-time WNCS, the status update data is usually of limited size and therefore transmitted with finite blocklength (FBL) [7]–[9], *e.g.*, 20-250 bytes [10]. Using FBL is expected to reduce AoI, while the inevitable block error probability (BLEP) may impair the AoI performance [7], compared to the infinite blocklength (IBL) scenario. Hence, it is necessary to investigate the impact of FBL on the information freshness of WNCSs to support real-time applications.

A. Related Work

Characterization and optimization of AoI: a) For observing the AoI during a certain time period, time-average AoI has been analyzed for random update systems [11], multi-server systems [12], [13] and multi-source systems [14], [15]. Subsequently, PAoI was analyzed for the $M/G/1$ queueing model [5]. In [16], retransmission and preemption policies were applied to reduce the average PAoI in the presence of BLEP. In [17], a practical truncated automatic repeat request (TARQ) scheme was adopted to strike the tradeoff between PAoI and energy. Apart from the time-average performance of AoI, variance of AoI [18] and PAoI outage probability [19] were proposed to indicate the fluctuation of AoI and account for extreme AoI events in real-time applications [19]. b) Regarding the AoI in the FBL regime, the normal approximation of achievable rate in the FBL regime was first derived [7], and the inevitable BLEP due to limits on channel coding was obtained over the additive white Gaussian noise (AWGN) channel. The impact of FBL on the AoI performance has been investigated for retransmissions [20], single-hop systems [21] and multi-sensor systems [22], where the blocklength adaptation was employed to minimize the average AoI. Our previous work analyzed the correlation between PAoI and delay in the FBL regime [23] and optimized them jointly [24]. In [25], the PAoI outage probability in the FBL regime was first characterized, based on which, the joint optimization of blocklength and transmit power was conducted under the constraint of AoI tail in [26]. The impact of FBL on the AoI tail was investigated in [27] for vehicular networks, where the AoI outage probability was minimized by blocklength adaptation. However, the aforementioned work focused on the communication system only, neglecting the interplay between AoI and sensing or control in WNCSs.

Sensing-aware or control-aware AoI in WNCSs: A typical WNCS has two types of wireless transmissions, *i.e.*, the sensor-controller and controller-actuator links. AoI and PAoI have been analyzed for WNCSs [28]–[36]. In [28] and [29], the estimation error was formulated as a function of age-penalty and AoI, respectively, where only the unreliable uplink (UL) was considered. Based on these, a WNCS with two-way delays was considered in [30] and [31], where the optimal joint sensor/controller waiting policy was proposed [30] and a stability-aware scheduling algorithm based on the communication and control co-design was provided [31]. In [32], an online transmission policy at the sensor was proposed to minimize remote estimation error based on the freshness-reliability tradeoff. Similar problem has been investigated in [33], where the controller decides whether to sample a new packet or attempt for retransmission. For WNCSs, the relationship between AoI and remote estimation error or control performance in the FBL regime was formulated in [34] and [35].

However, most of the aforementioned work on WNCSs [28]–[33] have assumed IBL, which can not be applied in real-time WNCSs directly. Also, only the average AoI performance was considered in the previous work on WNCSs, which is not sufficient to characterize the performance of real-time applications. Furthermore, UL and downlink (DL) are coupled in WNCSs, and the overall performance is affected by the packets of UL and DL in different manners. The aforementioned work analyzed the AoI in UL or DL only, or assumed one perfect link in WNCSs, neglecting the mutual impact of UL and DL. By extending the current AoI definition to take into consideration both UL and DL of the control loop in WNCSs, the age of loop (AoL) in the IBL regime was first analyzed in [36] and an AoL-based bandwidth allocation policy was proposed to minimize the WNCS cost. However, the balance between UL and DL, and their relationships with overall AoL performance in WNCSs with FBL have not been studied.

The following questions remain open:

- How is the average closed-loop AoL performance of WNCSs affected by the coupling between UL and DL in the FBL regime?
- What is the variance/outage probability of AoL affected by and how does it relate to the average AoL?
- How to bridge the gap between communication and control in WNCSs by AoL performances?

B. Contributions

Motivated by the open issues, in this paper, we investigate various peak AoL (PAoL) performances including the average, variance and outage probability, for WNCSs with FBL, and enable the co-design of communication and control. Our contributions are as follows[1].

- We characterize the average PAoL of WNCSs in relation to PAoI in UL and DL in the FBL regime. A closed-form expression for the average PAoL over fading channels is derived as a function of the blocklength and the maximum number of allowable transmissions in UL and DL, with the two-way delay and BLEP considered. It is proved that the average PAoL is less than the sum of UL PAoI and DL PAoI, due to the coupling of UL and DL. Also, their gap is proved to be independent of DL and increases monotonically with the sampling period and BLEP in UL. Our analytical results match the simulation results very well. In contrast, the previous work on the AoI analysis of WNCSs has investigated the average AoI in UL and DL separately [21], [28], [29], [32]–[35], or assumed IBL [28]–[33], [36], without considering BLEP.
- In addition to the average PAoL performance, we also provide an extensive analysis of the PAoL performance measured by variance and outage probability. Their closed-form expressions are derived and shown to be monotonically decreasing with blocklength and the maximum number of allowable transmissions in UL and DL. The variance and outage

[1]It is noteworthy that this paper is a substantive extension of our previous work in [1]. The main differences lie in that, 1) in addition to the average PAoL performance investigated in [1], the variance and the outage probability of PAoL are also investigated in this paper, and the relationship between the three performance metrics is analyzed; 2) a communication and control co-design is conducted by considering the three performance metrics, while only the average PAoL was considered in [1]; 3) extensive simulation results are presented in this paper, including the optimized variance and outage probability of PAoL as well as the variance and the outage probability of the control cost.

probability of PAoL demonstrate the same trend. Furthermore, there exists a tradeoff between the average and the variance/outage performance of PAoL with respect to blocklength (*i.e.*, transmission rate). However, the previous work on WNCSs [28]–[35] has focused on the average AoI performance, without considering the variance and outage probability of AoI.

- Based on the extensive performance analysis of PAoL, we conduct a PAoL-oriented communication and control co-design in WNCSs, via an effective blocklength adaptation scheme to minimize the average PAoL subject to the constraints on the variance and the outage probability of PAoL. In particular, the optimized maximum number of allowable transmissions and blocklengths in UL and DL are used in the control design and the corresponding average control cost is minimized and evaluated. To obtain this, the convexity and monotonicity of the average PAoL with respect to the blocklengths and the maximum number of allowable transmissions are analyzed, respectively. Simulation results show that the three PAoL performance metrics investigated are positively correlated with their control cost counterparts, and that the proposed PAoL-oriented optimization scheme significantly outperforms the UL only optimization scheme [29] and the DL only optimization scheme [21], with an up to 8-fold reduction in the average control cost.

The rest of the paper is organized as follows. The system model is presented in Section II. Closed-form expression of the average PAoL, as well as its relationship between UL PAoI and DL PAoI are derived in Section III. Variance of PAoL and PAoL outage probability are analyzed in Section IV. PAoL-oriented communication and control co-design is provided in Section V. Simulation results are given in Section VI, followed by conclusion in Section VII.

II. System Model

As shown in Fig. 1, we consider a single-loop WNCS, which consists of a dynamic unstable plant, an actuator, a wireless sensor, a remote controller and two unreliable channels (*i.e.*, sensor-to-controller and controller-to-actuator) [28]. We restrict our attention to the linear time-invariant (LTI) system, where the plant is monitored and controlled remotely over wireless links [28]. The operations are summarized as follows.

- The sensor takes periodic samples of the plant state with period T and transmits them to the controller through an unreliable wireless channel, inducing delay τ_{u} and transmission error ϵ_{u} [41]. It is assumed that update packets contain l_{u} bits of information encoded into m_{u} symbols with the modulation order Θ and symbol duration T_{s}.

- After receiving the sensor data, the event-triggered controller calculates the control messages that contain l_{d} bits of information encoded into m_{d} symbols with the modulation order Θ and symbol duration T_{s} [41], and transmits them to the actuator via wireless network, where the delay τ_{d} and transmission error ϵ_{d} are inevitable.
- The actuator takes an action based on the received control signals, and then the plant state is updated according to the control system dynamics.

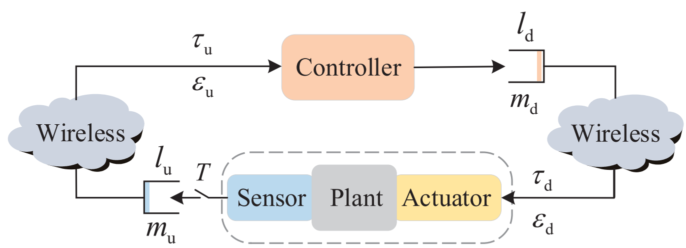

Fig. 1. System model of the single-loop WNCS.

In the following, the communication and control systems are introduced, respectively.

A. Communication System in the FBL Regime

In this paper, channels are assumed to experience quasi-static Rayleigh fading, where the channel gain h remains constant during one transmission period and varies independently among different transmission periods [17], [21]. The instantaneous SNR is given as $\gamma = \bar{\gamma}\left|h\right|^2$, where $\bar{\gamma} = \frac{P_{\mathrm{t}}}{\sigma^2}$ denotes the average SNR with the transmit power P_{t} and noise variance σ^2. Also, it is assumed that the TARQ retransmission policy, which requires low feedback overhead, is adopted [17], [21]. The source keeps transmitting the current status update repeatedly until the maximum number of allowable transmissions, r, is reached or the packet is transmitted successfully.

For analytical tractability, the normal approximations of achievable rate and BLEP in the FBL regime are employed[2] [7]. Therefore, with the blocklength m_α, the number of information bits l_α and a known instantaneous SNR γ, the BLEP ϵ_α can be expressed as

$$\epsilon_\alpha \approx Q\left(\sqrt{m_\alpha/V(\gamma)}\left(C(\gamma) - l_\alpha/m_\alpha\right)\right), \tag{1}$$

[2] It was illustrated in [38] that the Saddlepoint approximation is more accurate than the normal approximation in the case of extremely low BLEP, *e.g.*, 10^{-10}, but with no closed-form expression in general. As shown in [39], at a BLEP of 10^{-7}, the gap between the normal approximation and practical channel coding schemes is less than 0.1 dB. Thus, the normal approximation is considered to be a reasonable choice in system design [7], [20].

which is an upper bound on BLEP by neglecting the overhead of acquiring the instantaneous SNR [8]. Note that the subscript α is adopted for the notion simplicity, where $\alpha = \mathrm{u}$ and d denote the UL and DL, respectively. Specifically, the Q-function is given by $Q(x) = \int_x^\infty \frac{1}{\sqrt{2\pi}} e^{-t^2/2} dt$. $C(\gamma) = \ln(1+\gamma)$ denotes the channel capacity per channel use (c.u.) and $V(\gamma) = (1 - \frac{1}{(1+\gamma)^2})$ denotes the channel dispersion. Based on (1), the BLEP can be tightly approximated by transforming the Q-function into the form of segmented linear functions [21], *i.e.*,

$$\epsilon_\alpha(\gamma) \approx \begin{cases} 1, & \gamma < \delta_\alpha \\ \beta_\alpha(\gamma - \delta_\alpha) + 1/2, & \delta_\alpha \le \gamma < \delta_\alpha - \dfrac{1}{2\beta_\alpha} \\ 0, & \gamma > \delta_\alpha - \dfrac{1}{2\beta_\alpha}, \end{cases} \tag{2}$$

where $\delta_\alpha = e^{l_\alpha/m_\alpha} - 1$ and $\beta_\alpha = -\sqrt{\frac{m_\alpha}{2\pi(e^{2l_\alpha/m_\alpha}-1)}}$. Since the quasi-static fading channel is conditionally ergodic with respect to the channel realization h, the average BLEP is expressed as $\bar{\epsilon}_\alpha = \int_0^\infty f(\gamma)\epsilon_\alpha(\gamma) d\gamma$, where the probability density $f(\gamma)$ is an exponential function of SNR γ, as the channel gain h follows a complex Gaussian distribution with zero mean and unit variance. Based on (2), the average BLEP can be expressed as

$$\bar{\epsilon}_\alpha = \int_0^\infty \frac{1}{\bar{\gamma}} e^{-\frac{\gamma}{\bar{\gamma}}} \epsilon_\alpha(\gamma) d\gamma \approx 1 + \left(\beta_\alpha\bar{\gamma} - \beta_\alpha\bar{\gamma}e^{\frac{1}{2\beta_\alpha\bar{\gamma}}} - \frac{1}{2}\right) v_\alpha, \tag{3}$$

where $v_\alpha = e^{-\frac{\delta_\alpha}{\bar{\gamma}}}$.

B. LTI Control System

The considered LTI system is modeled as [41]

$$\dot{\mathbf{x}}(t) = \mathbf{A}\mathbf{x}(t) + \mathbf{B}\hat{\mathbf{u}}(t) + \mathbf{w}(t), \tag{4}$$

where $\mathbf{x}(t) \in \mathbb{R}^d$ is the plant state and d is the system dimension. $\hat{\mathbf{u}}(t) \in \mathbb{R}^q$ is the control signal and q is the control dimension. $\mathbf{w}(t)$ is the AWGN with zero mean and variance $\mathbf{R}_w$. Also, $\mathbf{A} \in \mathbb{R}^{d\times d}$ and $\mathbf{B} \in \mathbb{R}^{d\times q}$ are the constant system-transition and control-input matrixes, respectively. We assume that the plant state is sampled periodically by the sensor at times $t_n := nT$, $\forall n \in \mathbb{N}$. Letting subscript n denote the samples at t_n, the networked induced delays in UL and DL at time n are denoted by $\tau_{\mathrm{u},n}$ and $\tau_{\mathrm{d},n}$, respectively, depending on the number of transmission times and blocklengths. Then the total delay from the sensor to the actuator at time n is given by $\tau_n = \tau_{\mathrm{u},n} + \tau_{\mathrm{d},n}$, which is assumed to be bounded by one sampling period, *i.e.*, $\tau_n \le T$, allowing packets to arrive at the receiver in the correct order [41], [42]. Before the updated control messages are received, the actuator remains the last control input by using zero-order-holder and we have [42]

$$\hat{\mathbf{u}}(t) = \begin{cases} \hat{\mathbf{u}}_{n-1}, & t \in [t_n, t_n + \tau_n) \\ \hat{\mathbf{u}}_n, & t \in [t_n + \tau_n, t_{n+1}). \end{cases} \quad (5)$$

Then we conclude that

$$\mathbf{x}_{n+1} = e^{\mathbf{A}T}\mathbf{x}_n + \mathbf{\Gamma}_0^n \hat{\mathbf{u}}_n + \mathbf{\Gamma}_1^n \hat{\mathbf{u}}_{n-1} + \mathbf{w}_n, \quad (6)$$

where $\mathbf{\Gamma}_0^n = \int_0^{T-\tau_n} e^{\mathbf{A}t}\mathbf{B}dt$ and $\mathbf{\Gamma}_1^n = e^{\mathbf{A}(T-\tau_n)} \int_0^{\tau_n} e^{\mathbf{A}t}\mathbf{B}dt$. Let $p_\alpha = 1$ denote the event that the transmission in UL ($\alpha = \mathrm{u}$) or DL ($\alpha = \mathrm{d}$) is successful, whose probability is $1 - \epsilon_\alpha$. Also, we define $p_\alpha = 0$ as the event that the transmission is unsuccessful, with the probability of ϵ_α. Note that the actuator takes an action based on the previous control message in case of failed transmission [42]. Hence, the control input at time n is given by

$$\hat{\mathbf{u}}_n = p_{\mathrm{u,n}} p_{\mathrm{d,n}} \mathbf{u}_n + (1 - p_{\mathrm{u,n}} p_{\mathrm{d,n}}) \hat{\mathbf{u}}_{n-1}, \quad (7)$$

and the design of $\mathbf{u}_n$ is given in Subsection IV-B.

TABLE I

DEFINITIONS OF THE RELEVANT VARIABLES IN THE EVOLUTION OF INFORMATION AGE IN WNCSS

Variables	Definitions
α	$\alpha = \mathrm{u}$ and d denote UL and DL, respectively
m_α	m_u and m_d denote blocklength in UL and DL, respectively
l_α	l_u and l_d denote information size in UL and DL, respectively
ϵ_α	ϵ_u and ϵ_d denote BLEP in UL and DL, respectively
$\tau_{\alpha,n}$	$\tau_{\mathrm{u},n}$ and $\tau_{\mathrm{d},n}$ denote transmission delay in UL and DL, respectively
T_s	Symbol duration
Y_i	The arrival interval of two consecutive informative updates
S_i	The service time of the i-th informative packet
A_i	The instantaneous AoI achieved immediately before receiving the i-th informative packet
P_t, σ^2	Transmit power and noise variance
γ, $\bar{\gamma}$	Instantaneous SNR and average SNR
$\mathbf{x}(t)$, $\mathbf{x}_n$	Plant state in continuous time t and discrete time n
$\mathbf{u}(t)$, $\mathbf{u}_n$	Control input in continuous time t and discrete time n
$\mathbf{w}(t)$, $\mathbf{w}_n$	AWGN in continuous time t and discrete time n
T	Sampling period at the sensor
r	Maximum number of allowable transmissions

III. Average PAoL Analysis of WNCSs

In this section, the average information freshness performance of the WNCS is characterized. Recall that the total delay from the sensor to the actuator is assumed to be bounded by one sampling period, allowing packets to arrive at the receiver in the correct order. We present the closed-form expressions for the average PAoL $\bar{A}^{\mathrm{L}}$, UL PAoI $\bar{A}^{\mathrm{U}}$ and DL PAoI $\bar{A}^{\mathrm{D}}$. Based on these, their relationships are also analyzed.

A. Average PAoL of WNCSs

In Fig. 2, the control timeline and the corresponding evolution of AoI in the WNCS is shown. We consider a continuous-time status-update system, where blocklength can be relaxed to a continuous positive value and time t can take any positive value. The instantaneous AoI measures the elapsed time since the generation of the last successfully received packet, *i.e.*, $\Delta(t) = t - u(t)$, where $u(t)$ is the generation time of the latest update that is successfully received before time t. Since we focus on the loop performance, the instantaneous AoL drops when packets in UL and DL are both transmitted successfully, as shown in Fig. 2. It is assumed that the i-th update is generated at time g_i by the source (sensor) and successfully received by the destination (actuator) at time d_i. Then the service time of the i-th update in the loop can be expressed as $S_i^{\mathrm{L}} = d_i - g_i$, which characterizes the total transmission delay from the sensor to the actuator. Note that the impact of the fixed processing delay on the PAoL is neglected here, which can be integrated into the transmission delay. g_i^* denotes the packet that is not successfully received by the receiver due to the BLEP. In addition, we denote the interarrival time of two consecutive successfully-received informative packets by $Y_i^{\mathrm{L}} = g_i - g_{i-1}$, which is independent of the service time [4]. The PAoL for the i-th update is defined as the value of age achieved immediately before receiving the i-th packet, denoted by $A_i^{\mathrm{L}} = Y_i^{\mathrm{L}} + S_i^{\mathrm{L}}$. With the total number of successfully transmitted informative packets $N_{\mathcal{T}}$ over time interval $[0, \mathcal{T}]$, the average PAoL in the WNCS is given by [4]

$$\begin{aligned} \bar{A}^{\mathrm{L}} &= \lim_{\mathcal{T}\to\infty} \frac{1}{N_{\mathcal{T}}} \sum_{i=1}^{N_{\mathcal{T}}} A_i^{\mathrm{L}} = \lim_{\mathcal{T}\to\infty} \frac{1}{N_{\mathcal{T}}} \sum_{i=1}^{N_{\mathcal{T}}} (S_i^{\mathrm{L}} + Y_i^{\mathrm{L}}) \\ &\overset{(a)}{=} \mathbb{E}\left[S^{\mathrm{L}}\right] + \mathbb{E}\left[Y^{\mathrm{L}}\right], \end{aligned} \tag{8}$$

where (a) holds because of the assumed ergodicity of the stochastic process [3], and $\mathbb{E}[\cdot]$ denotes the expectation operator. To obtain the average PAoL in (8), we derive the average service time $\mathbb{E}\left[S^{\mathrm{L}}\right]$ and the average interarrival time $\mathbb{E}\left[Y^{\mathrm{L}}\right]$ as follows.

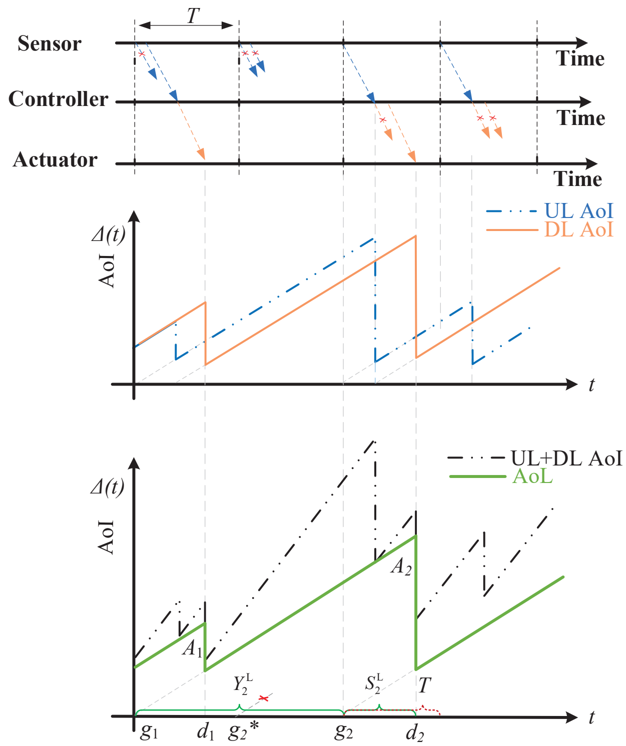

Fig. 2. Control timeline and the evolution of AoI in WNCSs, where UL AoI, DL AoI and AoL are shown.

With the average BLEP $\bar{\epsilon}_{\mathrm{u}}$ in UL and $\bar{\epsilon}_{\mathrm{d}}$ in DL, as well as the event that the packet is successfully transmitted within the maximum number of allowable transmissions r, the average service time is derived in Appendix A and given by

$$\mathbb{E}\left[S^{\mathrm{L}}\right]=\frac{m_{\mathrm{u}}T_{\mathrm{s}}}{1-\bar{\epsilon}_{\mathrm{u}}}-\frac{m_{\mathrm{u}}T_{\mathrm{s}}r\bar{\epsilon}_{\mathrm{u}}^{r}}{1-\bar{\epsilon}_{\mathrm{u}}^{r}}+\frac{m_{\mathrm{d}}T_{\mathrm{s}}}{1-\bar{\epsilon}_{\mathrm{d}}}-\frac{m_{\mathrm{d}}T_{\mathrm{s}}r\bar{\epsilon}_{\mathrm{d}}^{r}}{1-\bar{\epsilon}_{\mathrm{d}}^{r}}. \tag{9}$$

Also, the average interarrival time is derived in Appendix A and given by

$$\mathbb{E}\left[Y^{\mathrm{L}}\right]=\frac{T}{(1-\bar{\epsilon}_{\mathrm{u}}^{r})(1-\bar{\epsilon}_{\mathrm{d}}^{r})}. \tag{10}$$

Based on (9) and (10), the average PAoL in a WNCS is given in Theorem 1.

Theorem 1: *The average PAoL in a WNCS is formulated as a function of UL blocklength m_u and DL blocklength m_d, as well as the maximum number of allowable transmissions, r, given by*

$$\bar{A}^{\mathrm{L}}=\frac{T}{(1-\bar{\epsilon}_{\mathrm{u}}^{r})(1-\bar{\epsilon}_{\mathrm{d}}^{r})}+\left[\frac{m_{\mathrm{u}}(1-r\bar{\epsilon}_{\mathrm{u}}^{r}-\bar{\epsilon}_{\mathrm{u}}^{r}+r\bar{\epsilon}_{\mathrm{u}}^{r+1})}{(1-\bar{\epsilon}_{\mathrm{u}})(1-\bar{\epsilon}_{\mathrm{u}}^{r})}+\frac{m_{\mathrm{d}}(1-r\bar{\epsilon}_{\mathrm{d}}^{r}-\bar{\epsilon}_{\mathrm{d}}^{r}+r\bar{\epsilon}_{\mathrm{d}}^{r+1})}{(1-\bar{\epsilon}_{\mathrm{d}})(1-\bar{\epsilon}_{\mathrm{d}}^{r})}\right]T_{\mathrm{s}}, \tag{11}$$

which is monotonically decreasing with r. Without retransmission, i.e., $r=1$, (11) reduces to

$$\bar{A}_{\mathrm{s}}^{\mathrm{L}}=\frac{T}{(1-\bar{\epsilon}_{\mathrm{u}})(1-\bar{\epsilon}_{\mathrm{d}})}+(m_{\mathrm{u}}+m_{\mathrm{d}})T_{\mathrm{s}}. \tag{12}$$

Proof: Please refer to Appendix A. ■

Theorem 1 shows that the average PAoL is dependent on the blocklengths in UL and DL, and that retransmission reduces the average PAoL. This is due to the fact that retransmission reduces the interarrival time but leads to an increased service time. Also, the interarrival time dominates the overall PAoL performance, based on the fact that the sampling period is larger than the networked delay in a transmission round, *i.e.*, $T > r(m_{\mathrm{u}} + m_{\mathrm{d}})T_{\mathrm{s}}$, as shown in Fig. 2.

Equation (11) also confirms that a lower BLEP leads to a lower average PAoL. The average BLEP $\bar{\epsilon}_\alpha \in (0, 0.5)$ is true for the typical real-time applications [40], based on which, Corollary 1 shows the range of the average PAoL.

Corollary 1: *With average BLEP $\bar{\epsilon}_\alpha \in (0, 0.5)$, the lower and upper bounds on the average PAoL are given by $\bar{A}^{\mathrm{L}}_{\text{lower}} = T + (m_{\mathrm{u}} + m_{\mathrm{d}})T_{\mathrm{s}}$ and $\bar{A}^{\mathrm{L}}_{\text{upper}} = \frac{T}{(1-0.5^r)^2} + (2 - \frac{r}{2^r - 1})(m_{\mathrm{u}} + m_{\mathrm{d}})T_{\mathrm{s}}$, respectively.*

Proof: Based on Lemma 1, substituting $\bar{\epsilon}_{\mathrm{u}} = 0$ and $\bar{\epsilon}_{\mathrm{d}} = 0$ into (11) yields the lower bound $\bar{A}^{\mathrm{L}}_{\text{lower}}$. In addition, substituting $\bar{\epsilon}_{\mathrm{u}} = 0.5$ and $\bar{\epsilon}_{\mathrm{d}} = 0.5$ into (11) yields the upper bound $\bar{A}^{\mathrm{L}}_{\text{upper}}$. ■

From Corollary 1, we have the following observations: (1) When $r = 1$, *i.e.*, no re-transmission is allowed, we have $T + (m_{\mathrm{u}} + m_{\mathrm{d}})T_{\mathrm{s}} \le \bar{A}^{\mathrm{L}} \le 4T + (m_{\mathrm{u}} + m_{\mathrm{d}})T_{\mathrm{s}}$. (2) when $r \to \infty$, *i.e.*, allowing re-transmission until successful decoding with the constraint of sampling period, we have $T + (m_{\mathrm{u}} + m_{\mathrm{d}})T_{\mathrm{s}} \le \bar{A}^{\mathrm{L}} \le T + 2(m_{\mathrm{u}} + m_{\mathrm{d}})T_{\mathrm{s}}$. (3) The impact of UL and DL on the average PAoL are coupled through interarrival time and drives the analysis of the relationship among PAoL, UL PAoI and DL PAoI.

B. PAoL vs. UL PAoI and DL PAoI

Based on Subsection III-A, the average PAoI in UL and in DL can be derived in a similar way. Then the relationship among PAoL, UL PAoI and DL PAoI is shown in Theorem 2.

Theorem 2: *The average PAoL $\bar{A}^L$ is the sum of the UL and DL average PAoI, $\bar{A}^U$ and $\bar{A}^D$, with the average UL interarrival time removed, given by*

$$\bar{A}^{\mathrm{L}} = \bar{A}^{\mathrm{D}} + \bar{A}^{\mathrm{U}} - \frac{T}{1 - \bar{\epsilon}_{\mathrm{u}}^r}, \tag{13}$$

where

$$\bar{A}^{\mathrm{U}} = \frac{T}{1 - \bar{\epsilon}_{\mathrm{u}}^r} + \frac{m_{\mathrm{u}} T_{\mathrm{s}} (1 - r\bar{\epsilon}_{\mathrm{u}}^r - \bar{\epsilon}_{\mathrm{u}}^r + r\bar{\epsilon}_{\mathrm{u}}^{r+1})}{(1 - \bar{\epsilon}_{\mathrm{u}})(1 - \bar{\epsilon}_{\mathrm{u}}^r)}, \tag{14}$$

and

$$\bar{A}^{\mathrm{D}} = \frac{T}{(1 - \bar{\epsilon}_{\mathrm{u}}^r)(1 - \bar{\epsilon}_{\mathrm{d}}^r)} + \frac{m_{\mathrm{d}} T_{\mathrm{s}} (1 - r\bar{\epsilon}_{\mathrm{d}}^r - \bar{\epsilon}_{\mathrm{d}}^r + r\bar{\epsilon}_{\mathrm{d}}^{r+1})}{(1 - \bar{\epsilon}_{\mathrm{d}})(1 - \bar{\epsilon}_{\mathrm{d}}^r)}. \tag{15}$$

■

Theorem 2 proves that the average PAoL is less than the sum of UL PAoI and DL PAoI, and that they are affected by blocklengths in UL and DL in a different manner. This is due to the fact that AoL is destination-centric. Hence, the average interarrival time in UL is removed in the overall PAoL performance. Also, it is concluded that UL and DL are coupled in the average PAoL with an unreliable UL channel and demonstrates the necessity of introducing the average PAoL. Then we introduce Corollary 2 to quantify the coupling between PAoL and UL PAoI as well as DL PAoI.

Corollary 2: *The gap between PAoL and the sum of UL PAoI and DL PAoI,* $G = (\bar{A}^D + \bar{A}^U) - \bar{A}^L = \frac{T}{1-\bar{\epsilon}_u^T}$*, is adopted to quantify the coupling, which is increasing with respect to the sampling period and BLEP in UL. Due the existence of this gap, minimizing the sum of average UL PAoI and DL PAoI is not equivalent to minimizing the average PAoL in the FBL regime.*

Proof: Please refer to Appendix B. ■

Corollary 2 shows that the gap between PAoL and the sum of UL PAoI and DL PAoI depends on the sampling period and BLEP of UL. This is due to the fact that the controller is event-triggered and the DL can only transmit when the UL packets have been successfully received by the controller. Hence, UL has a more significant impact on the overall performance with the higher sampling period and BLEP. As shown in Fig. 2, only when UL packets are received by the controller successfully, DL packets can be transmitted. Therefore, it is proved in Appendix B that the average DL PAoI is affected by both blocklengths in UL and DL, and is monotonically decreasing with respect to the blocklength m_{u} in UL if $l_{\mathrm{u}} \geq \pi$.

IV. Variance of PAoL and PAoL outage Probability

In Section III, the average PAoL is analyzed, which falls short in properly characterizing the information freshness of real-time applications in WNCSs as it does not reflect the fluctuating and extreme events. Hence, in this section, the variance and the outage probability of PAoL are derived and their properties are investigated to provide an extensive analysis of the PAoL performance. The results will be applied in the communication and control co-design in Section V.

A. Variance of PAoL

In this subsection, we investigate the variance of PAoL, which quantifies the stability of the worst information freshness at the receiver. From (8), the variance of PAoL can be obtained by $\mathrm{Var}[A^{\mathrm{L}}] = \mathrm{Var}[Y^{\mathrm{L}}] + \mathrm{Var}[S^{\mathrm{L}}]$, due to the independence of the interarrival time Y^{L} and service time S^{L}. Based on the fact that $\mathrm{Var}[Y^{\mathrm{L}}] = \mathbb{E}[{Y^{\mathrm{L}}}^2] - \mathbb{E}[Y^{\mathrm{L}}]^2$, where $\mathbb{E}[{Y^{\mathrm{L}}}^2]$ and $\mathbb{E}[Y^{\mathrm{L}}]^2$ are derived in Appendix C, the variance of interarrival time can be expressed as

$$\mathrm{Var}[Y^{\mathrm{L}}] = \frac{T^2(\bar{\epsilon}_{\mathrm{u}}^r + \bar{\epsilon}_{\mathrm{d}}^r - \bar{\epsilon}_{\mathrm{u}}^r \bar{\epsilon}_{\mathrm{d}}^r)}{(1-\bar{\epsilon}_{\mathrm{u}}^r)^2(1-\bar{\epsilon}_{\mathrm{d}}^r)^2}. \tag{16}$$

By deriving $\mathrm{Var}[S^{\mathrm{L}}] = \mathbb{E}[{S^{\mathrm{L}}}^2] - \mathbb{E}[S^{\mathrm{L}}]^2$ in Appendix C, the variance of service time can be expressed as

$$\mathrm{Var}[S^{\mathrm{L}}] = \frac{m_{\mathrm{u}}^2 T_{\mathrm{s}}^2 \bar{\epsilon}_{\mathrm{u}}}{(1-\bar{\epsilon}_{\mathrm{u}})^2} - \frac{m_{\mathrm{u}}^2 T_{\mathrm{s}}^2 r^2 \bar{\epsilon}_{\mathrm{u}}^r}{(1-\bar{\epsilon}_{\mathrm{u}}^r)^2} + \frac{m_{\mathrm{d}}^2 T_{\mathrm{s}}^2 \bar{\epsilon}_{\mathrm{d}}}{(1-\bar{\epsilon}_{\mathrm{d}})^2} - \frac{m_{\mathrm{d}}^2 T_{\mathrm{s}}^2 r^2 \bar{\epsilon}_{\mathrm{d}}^r}{(1-\bar{\epsilon}_{\mathrm{d}}^r)^2}. \tag{17}$$

Based on (16) and (17), the variance of PAoL can be derived, as shown in Theorem 3.

Theorem 3: *The variance of PAoL in a WNCS is formulated as a function of UL blocklength m_u and DL blocklength m_d, and the maximum number of allowable transmissions, r, given by*

$$\mathrm{Var}[A^{\mathrm{L}}] = \frac{T^2(\bar{\epsilon}_{\mathrm{u}}^r + \bar{\epsilon}_{\mathrm{d}}^r - \bar{\epsilon}_{\mathrm{u}}^r \bar{\epsilon}_{\mathrm{d}}^r)}{(1-\bar{\epsilon}_{\mathrm{u}}^r)^2(1-\bar{\epsilon}_{\mathrm{d}}^r)^2} + \left[\frac{m_{\mathrm{u}}^2 \bar{\epsilon}_{\mathrm{u}}}{(1-\bar{\epsilon}_{\mathrm{u}})^2} - \frac{m_{\mathrm{u}}^2 r^2 \bar{\epsilon}_{\mathrm{u}}^r}{(1-\bar{\epsilon}_{\mathrm{u}}^r)^2} + \frac{m_{\mathrm{d}}^2 \bar{\epsilon}_{\mathrm{d}}}{(1-\bar{\epsilon}_{\mathrm{d}})^2} - \frac{m_{\mathrm{d}}^2 r^2 \bar{\epsilon}_{\mathrm{d}}^r}{(1-\bar{\epsilon}_{\mathrm{d}}^r)^2}\right] T_{\mathrm{s}}^2, \tag{18}$$

which is monotonically decreasing with respect to r. Without retransmission, i.e., $r=1$, the variance of PAoL in a WNCS is given by

$$\mathrm{Var}[A_{\mathrm{s}}^{\mathrm{L}}] = \frac{T^2(\bar{\epsilon}_{\mathrm{u}} + \bar{\epsilon}_{\mathrm{d}} - \bar{\epsilon}_{\mathrm{u}} \bar{\epsilon}_{\mathrm{d}})}{(1-\bar{\epsilon}_{\mathrm{u}})^2(1-\bar{\epsilon}_{\mathrm{d}})^2}. \tag{19}$$

Proof: Please refer to Appendix C. ■

Theorem 3 shows that the variance of PAoL is affected by the maximum number of allowable transmissions and blocklengths in UL and DL significantly. Without retransmission, the variance of PAoL depends on the variance of interarrival time, and is independent of service time. Also, the variances of UL PAoI and DL PAoI can be derived in a similar way, which shows that the variance of PAoL is less than the sum of the variances of UL PAoI and DL PAoI.

Based on (18), it is concluded that with a lower BLEP, a lower variance of PAoL can be obtained. Then Corollary 3 shows the range of variance of PAoL.

Corollary 3: *With a reasonable average BLEP $\bar{\epsilon}_\alpha \in (0, 0.5)$, the range of variance of PAoL is given by* $\mathrm{Var}[A^L] \in \left(0, \frac{T^2(2*0.5^r+0.5^{2r})}{(1-0.5^r)^4} + \left[2m_u^2 - \frac{m_u^2 r^2 0.5^r}{(1-0.5^r)^2} + 2m_d^2 - \frac{m_d^2 r^2 0.5^r}{(1-0.5^r)^2}\right] T_s^2\right)$. ■

Corollary 3 implies that the upper bound on the variance of PAoL is lower than $20T^2$ when $r=1$, and larger than $(2m_{\mathrm{u}}^2 + 2m_{\mathrm{d}}^2)T_{\mathrm{s}}^2$ when $r \to \infty$. Based on Theorems 1 and 3, the relationship between the average PAoL and variance of PAoL can be derived in Corollary 4.

Corollary 4: *The average PAoL can be derived as a function of the variance of PAoL, given by*

$$\bar{A}^{\mathrm{L}}=\frac{\sqrt{\mathrm{Var}[A^{\mathrm{L}}]-\mathrm{Var}[S^{\mathrm{L}}]}}{\bar{\epsilon}_{\mathrm{u}}^{r}+\bar{\epsilon}_{\mathrm{d}}^{r}-\bar{\epsilon}_{\mathrm{u}}^{r}\bar{\epsilon}_{\mathrm{d}}^{r}}+\frac{m_{\mathrm{u}}T_{\mathrm{s}}(1-(r+1)\bar{\epsilon}_{\mathrm{u}}^{r}+r\bar{\epsilon}_{\mathrm{u}}^{r+1})}{(1-\bar{\epsilon}_{\mathrm{u}})(1-\bar{\epsilon}_{\mathrm{u}}^{r})}+\frac{m_{\mathrm{d}}T_{\mathrm{s}}(1-(r+1)\bar{\epsilon}_{\mathrm{d}}^{r}+r\bar{\epsilon}_{\mathrm{d}}^{r+1})}{(1-\bar{\epsilon}_{\mathrm{d}})(1-\bar{\epsilon}_{\mathrm{d}}^{r})}. \tag{20}$$

Without retransmission, i.e., $r=1$, *(20) reduces to (21)*

$$\bar{A}_{\mathrm{s}}^{\mathrm{L}}=\frac{\mathrm{Std}[A_{\mathrm{s}}^{\mathrm{L}}]}{\bar{\epsilon}_{\mathrm{u}}+\bar{\epsilon}_{\mathrm{d}}-\bar{\epsilon}_{\mathrm{u}}\bar{\epsilon}_{\mathrm{d}}}+(m_{\mathrm{u}}+m_{\mathrm{d}})T_{s}, \tag{21}$$

where $\mathrm{Std}[A_{\mathrm{s}}^{\mathrm{L}}]=\sqrt{\mathrm{Var}[A_{\mathrm{s}}^{\mathrm{L}}]}$ denotes the standard deviation of PAoL. ■

Corollary 4 shows that the relationship between the average PAoL and variance of PAoL is complex, which is shown in detail in Section VI.

B. PAoL outage Probability

In this subsection, the PAoL outage probability is analyzed, which characterizes the probability that PAoL exceeds a desired threshold δ, *i.e.*, $\Pr[A^{\mathrm{L}}>\delta]=\lim_{i\to\infty}\Pr[A_{i}^{\mathrm{L}}>\delta]$, where A_{i}^{L} denotes the i-th instantaneous PAoL. Based on the steady-state PAoL distribution, the closed-form expression for the PAoL outage probability is shown in Theorem 4.

Theorem 4: *The PAoL outage probability in a WNCS is formulated as*

$$\Pr[A^{\mathrm{L}}>\delta]=\sum_{r_{\mathrm{u}}=1}^{r}\sum_{r_{\mathrm{d}}=1}^{r}\frac{\chi^{\phi-1}}{1-\chi}(1-\bar{\epsilon}_{\mathrm{u}})(1-\bar{\epsilon}_{\mathrm{d}})\bar{\epsilon}_{\mathrm{u}}^{r_{\mathrm{u}}-1}\bar{\epsilon}_{\mathrm{d}}^{r_{\mathrm{d}}-1}, \tag{22}$$

where $\chi=(1-(1-\bar{\epsilon}_{u}^{r})(1-\bar{\epsilon}_{d}^{r}))$ *and* $\phi=\lceil\frac{\delta-r_{u}m_{u}T_{s}-r_{d}m_{d}T_{s}}{T}\rceil$. r_u *and* r_d *denote the index of transmission times for UL and DL, respectively. Also, the PAoL outage probability is a decreasing function of the maximum number of allowable transmissions. Without retransmission, i.e.,* $r=1$, *the PAoL outage probability in a WNCS is given by*

$$\Pr[\mathrm{A}_{\mathrm{s}}^{\mathrm{L}}>\delta]=\chi_{\mathrm{s}}^{\phi_{\mathrm{s}}-1}, \tag{23}$$

where $\chi_{\mathrm{s}}=(1-(1-\bar{\epsilon}_{\mathrm{u}})(1-\bar{\epsilon}_{\mathrm{d}}))$ and $\phi_{\mathrm{s}}=\lceil\frac{\delta-m_{\mathrm{u}}T_{\mathrm{s}}-m_{\mathrm{d}}T_{\mathrm{s}}}{T}\rceil$.

Proof: Please refer to Appendix D. ■

Since PAoL is larger than the sampling period, (22) reduces to (24) when the PAoL threshold is an integer times of the sampling period, as shown in Corollary 5.

Corollary 5: *If PAoL threshold is an integer times of the sampling period, i.e.,* $\delta \bmod T=0$, *the PAoL outage probability is formulated as an exponential function of threshold* δ, *given by*

$$\Pr[\mathrm{A}^{\mathrm{L}}>\delta]=\chi^{\frac{\delta}{\mathrm{T}}-1}. \tag{24}$$

Proof: When $\delta \bmod T = 0$, $\phi = \lceil \frac{\delta - r_{\rm u} m_{\rm u} T_{\rm s} - r_{\rm d} m_{\rm d} T_{\rm s}}{T} \rceil$ can be simplified as $\phi = \frac{\delta}{T}$. Applying the series expansions $\sum_{r_{\rm u}=1}^{r}(1-\bar{\epsilon}_{\rm u})\bar{\epsilon}_{\rm u}^{r_{\rm u}-1} = 1-\bar{\epsilon}_{\rm u}^{r}$ and $\sum_{r_{\rm d}=1}^{r}(1-\bar{\epsilon}_{\rm d})\bar{\epsilon}_{\rm d}^{r_{\rm d}-1} = 1-\bar{\epsilon}_{\rm d}^{r}$, the PAoL outage probability is given by $\Pr[{\rm A}^{\rm L} > \delta] = \chi^{\frac{\delta}{\rm T}-1}$. ■

With a lower BLEP, the average PAoL is lower and hence the PAoL outage probability is reduced, based on which, the range of PAoL outage probability is shown in Corollary 6.

Corollary 6: *With a reasonable average BLEP* $\bar{\epsilon}_{\alpha} \in (0, 0.5)$, *the range of PAoL outage probability is given by* $\Pr[{\rm A}^{L} > \delta] \in \left(0, [1-(1-0.5^{\rm r})^2]^{\frac{\delta}{\rm T}-1}\right)$. ■

Based on Theorem 5 and Corollary 6, it is concluded that without retransmission, the upper bound on the PAoL outage probability is lower than $0.75^{\frac{\delta}{T}-1}$.

C. Summary

Based on the analysis in Sections III and IV, the range of PAoL can be summarized in Table II, where $\bar{A}^{\rm L}_{\rm lower} = T + (m_{\rm u} + m_{\rm d})T_{\rm s}$, $\bar{A}^{\rm L}_{\rm upper} = \frac{T}{(1-0.5^r)^2} + (2 - \frac{r}{2^r-1})(m_{\rm u}+m_{\rm d})T_{\rm s}$, $\Pr[A^{\rm L} > \delta]_{\rm upper} = [1-(1-0.5^r)^2]^{\frac{\delta}{T}-1}$ and $\mathrm{Var}[A^{\rm L}]_{\rm upper} = \frac{T^2(2*0.5^r+0.5^{2r})}{(1-0.5^r)^4} + \left[2m_{\rm u}^2 - \frac{m_{\rm u}^2 r^2 0.5^r}{(1-0.5^r)^2} + 2m_{\rm d}^2 - \frac{m_{\rm d}^2 r^2 0.5^r}{(1-0.5^r)^2}\right] T_{\rm s}^2$. It is concluded that the upper and lower bounds on the average PAoL depend on the sampling period and blocklengths in UL and DL. Due to the fact that the variance of PAoL and PAoL outage are induced by unreliable transmissions, the lower bounds on the variance of PAoL and PAoL outage are zero with error-free transmission. Also, it is shown that with retransmissions, the upper bounds on the average PAoL, variance of PAoL and PAoL outage probability are reduced, thanks to the enhanced reliability, as proved in Theorems 1, 3 and 4.

TABLE II

INFORMATION FRESHNESS ANALYSIS OF WNCSS

Performance metric	Transmission times r	$r=1$ (No retransmission)	$r=2$ (One retransmission)
Average PAoL $\bar{A}^{\rm L}$	$\left(\bar{A}^{\rm L}_{\rm lower}, \bar{A}^{\rm L}_{\rm upper}\right)$	$\left(\bar{A}^{\rm L}_{\rm lower}, 4T + (m_{\rm u}+m_{\rm d})T_{\rm s}\right)$	$\left(\bar{A}^{\rm L}_{\rm lower}, 1.8T + 1.3(m_{\rm u}+m_{\rm d})T_{\rm s}\right)$
Variance of PAoL $\mathrm{Var}[A^{\rm L}]$	$\left(0, \mathrm{Var}[A^{\rm L}]_{\rm upper}\right)$	$\left(0, 20T^2\right)$	$\left(0, 1.8T^2 + 0.2(m_{\rm u}^2 + m_{\rm d}^2)T_{\rm s}^2\right)$
PAoL outage probability $\Pr[A^{\rm L} > \delta]$	$\left(0, \Pr[A^{\rm L} > \delta]_{\rm upper}\right)$	$\left(0, 0.75^{\frac{\delta}{T}-1}\right)$	$\left(0, 0.4^{\frac{\delta}{T}-1}\right)$

V. PAoL-oriented Communication and Control Co-Design

In Sections III and IV, the average, variance and outage PAoL performances in WNCSs are analyzed. This section aims to minimize the average PAoL in the WCNS with the constraints on the variance of PAoL and PAoL outage probability by optimizing the blocklengths in UL and DL. Based on these, the optimal feedback control is also designed to attain an optimized co-design of communication and control.

A. PAoL-oriented blocklength Adaptation with Retransmission

Based on the analysis in Section IV, it is concluded that retransmission is beneficial to improve the average PAoL, variance and outage probability of PAoL performances. Hence, the optimal maximum number of allowable transmissions is obtained at its maximum allowable value, *i.e.*, $r^* = r_{\max}$. To ensure the various PAoL performances of WNCSs, we aim to minimize the average PAoL subject to the variance of PAoL and PAoL outage probability by jointly optimizing the blocklength vector $\mathbf{m} = [m_{\mathrm{u}}, m_{\mathrm{d}}]$.

$$
\begin{aligned}
\textbf{P1}: \quad & \min_{\mathbf{m}} \quad \bar{A}^{\mathrm{L}} && (25)\\
\text{s.t.} \quad & (C1): l_\alpha / \log_2 \Theta \le m_\alpha \le m_{\alpha,\max}, m_\alpha \in \mathbb{N}_+,\\
& (C2): \mathrm{Var}[A^{\mathrm{L}}] \le \mathrm{V}_{\max},\\
& (C3): \Pr[A^{\mathrm{L}} > \delta] \le \Pr_{\max},
\end{aligned}
$$

where (C1) constraints the minimum blocklength that depends on the number of information bits l_α and modulation order Θ, and the maximum allowable blocklength $m_{\alpha,\max}$. (C2) and (C3) limit the maximum allowable PAoL variance $V_{\max}$ and outage probability $\Pr_{\max}$, respectively.

First, we relax the integer constraint (C1) into continuous space. Then Propositions 1$\sim$3 are presented to address this optimization problem.

Proposition 1: *The average PAoL $\bar{A}^L$ is convex with respect to blocklength vector* **m**, *if $l_\alpha \ge \pi$ and $\bar{\epsilon}_\alpha \le 0.5$.*

Proof: Please refer to the Appendix E. ■

Proposition 1 implies that there exist optimal blocklengths that minimize the average PAoL, based on which the blocklength adaptation is conducted.

Proposition 2: *The variance of PAoL $\mathrm{Var}[A^{\mathrm{L}}]$ and the outage probability of PAoL $\Pr[A^L > \delta]$ are monotonically decreasing with respect to the blocklength vector* **m**.

Proof: Please refer to Appendix F. ■

Proposition 2 implies that lower variance of PAoL and PAoL outage probability can be obtained by a larger blocklength. This is due to that a larger blocklength leads to a lower BLEP, results in a smaller interarrival time, which dominates the variance of PAoL and PAoL outage probability. Based on Propositions 1 and 2, it is concluded that there is a tradeoff between the average PAoL and the variance/outage probability of PAoL with respect to blocklength.

TABLE III

PROPERTIES ANALYSIS OF AVERAGE PAOL, VARIANCE OF PAOL AND PAOL OUTAGE PROBABILITY IN WNCSS

Performance metric	Performance vs. blocklength
Average PAoL	Convex
Variance of PAoL	Mono-decreasing
PAoL outage probability	Mono-decreasing

The properties of average PAoL, variance of PAoL and PAoL outage probability with respect to the blocklengths are summarized in Table III, which demonstrates that **P1** is a convex optimization problem in its admissible set based on Propositions 1$\sim$2. To handle **P1**, we propose a PAoL-oriented blocklength adaptation scheme with retransmission policy, where the optimal blocklengths are obtained based on Newton's method that achieves a superlinear convergence rate and has relatively low complexity [21]. Proposition 2 shows that there exist minimum blocklengths $m_{\alpha,\min}^{\mathrm{V}}$ that satisfies (C2), given by $m_{\alpha,\min}^{\mathrm{V}} = \min\{m_\alpha | \mathrm{Var}[A^{\mathrm{L}}(m_\alpha)] \leq V_{\max}\}$. Also, there exist minimum blocklengths $m_{\alpha,\min}^{\delta} = \min\{m_\alpha | \Pr[\mathrm{A}^{\mathrm{L}}(\mathrm{m}_\alpha) > \delta] \leq \Pr_{\max}\}$ that satisfies (C4) based on Proposition 3. To ensure that the selected blocklengths are able to meet constraints (C1)$\sim$(C3), a 'max' operation is performed, *i.e.*, $m_{\alpha,\min} = \max\{l_\alpha / \log_2 \Theta, m_{\alpha,\min}^{\mathrm{V}}, m_{\alpha,\min}^{\delta}\}$. Therefore, the optimal blocklengths can be obtained in Theorem 5.

Theorem 5: *The optimal UL and DL blocklengths that minimize the average PAoL with the constraints on the transmitted information bits, variance of PAoL and PAoL outage probability can be expressed as*

$$m_\alpha^* = \begin{cases} m_{\alpha,\min}, & m_\alpha^\dagger \leq m_{\min}, \\ \underset{m_\alpha \in (\lfloor m_\alpha^\dagger \rfloor, \lceil m_\alpha^\dagger \rceil)}{\arg\min} \bar{A}^{\mathrm{L}}, & m_{\alpha,\min} \leq m_\alpha^\dagger \leq m_{\max}, \\ m_{\alpha,\max}, & m_{\alpha,\max} \leq m_\alpha^\dagger, \end{cases} \tag{26}$$

where $m_\alpha^\dagger$ is the root of $\nabla \bar{A}^L(m_u, m_d) = 0$. ■

The blocklength adaptation with retransmission scheme is summarized in Algorithm 1.

Algorithm 1: blocklength Adaptation with Retransmission

---

1 **Input:** Maximum allowable blocklength $m_{\alpha,\max}$, maximum allowable variance of PAoL $V_{\max}$, maximum allowable PAoL outage probability $\Pr_{\max}$, information bits l_α, initial point (m_{u_0}, m_{d_0}), error tolerance ξ.

2 Obtain the optimal blocklength vector $\mathbf{m}^*$ based on Newton's method in (26).

3 **Output:** Optimal blocklength vector $\mathbf{m}^*$.

Note that UL PAoI-oriented and UL PAoI-oriented schemes can be obtained by a similar method and adopted as benchmarks, which are omitted due to limited space.

B. Optimal Feedback Control Design

Based on the optimized blocklengths $\mathbf{m}^*$ derived in Subsection IV-A, the corresponding BLEP can be obtained as ϵ_α^* and used in the control design. Recall that the actuator takes an action based on the previous control message in case of failed transmission [42]. Also, τ_n and $\hat{\mathbf{u}}_n$ can be updated based on Subsection II-B. Then, we introduce an augmented discrete-time state variable $\mathbf{z}_n = [\mathbf{x}_n \quad \hat{\mathbf{u}}_{n-1}]^\top$ to analyze the system, which can be further expressed as

$$\mathbf{z}_{n+1} = \mathbf{\Phi}(T, \tau_n)\mathbf{z}_n + \mathbf{\Gamma}(T, \tau_n)\hat{\mathbf{u}}_n + \mathbf{w}_n, \tag{27}$$

where $\mathbf{\Phi}(T, \tau_n) = \begin{bmatrix} e^{\mathbf{A}T} & \mathbf{\Gamma}_1^n \\ 0 & 0 \end{bmatrix}$ and $\mathbf{\Gamma}(T, \tau_n) = \begin{bmatrix} \mathbf{\Gamma}_0^n \\ I \end{bmatrix}$.

Particularly, the control performance is considered and defined as the reciprocal of linear-quadratic regulator control cost, which is given by [41]

$$J = \mathbb{E}\{\sum_{n=0}^{N-1}[\mathbf{z}_n^\top \mathbf{Q}\mathbf{z}_n + \hat{\mathbf{u}}_n^\top R\hat{\mathbf{u}}_n] + \mathbf{z}_N^\top \mathbf{Q}\mathbf{z}_N\}, \tag{28}$$

where $\mathbf{Q}$ and R are positive defined weight factors. Then, the optimal control law is designed to minimize the control cost, given by $\mathbf{u}_n = -\mathbf{K}\mathbf{z}_n$ [42], where $\mathbf{K}$ is the control gain given by $\mathbf{K} = (R + \mathbf{\Gamma}^\top\mathbf{P}\mathbf{\Gamma})^{-1}\mathbf{\Gamma}^\top\mathbf{P}\mathbf{\Phi}$ and $\mathbf{P}$ is the steady-state solution of the control Riccati recursion $\mathbf{P} = \mathbf{\Phi}^\top\mathbf{P}\mathbf{\Phi} - (\mathbf{\Phi}^\top\mathbf{P}\mathbf{\Gamma})(\mathbf{\Gamma}^\top\mathbf{P}\mathbf{\Gamma} + R)^{-1}(\mathbf{\Gamma}^\top\mathbf{P}\mathbf{\Phi}) + \boldsymbol{Q}$ [41].

VI. Simulation Results

In this section, we first verify the derived average PAoL, variance and outage probability of PAoL expressions and their properties via Monte Carlo simulations, where 100,000 packets are generated. Then, the performance of the proposed PAoL-oriented blocklength adaptation scheme with retransmission is demonstrated. Following [41], we consider an unstable and controllable plant in the form of (1) with $\mathbf{A} = \begin{bmatrix} 8 & 1 \\ 0 & 5 \end{bmatrix}$, $\mathbf{B} = \begin{bmatrix} 0 \\ 2 \end{bmatrix}$, $\mathbf{C} = \begin{bmatrix} 1 & 0 \\ 0 & 1 \end{bmatrix}$, $\mathbf{Q} = \mathbf{I}$ and $R = 0.1$. Considering a typical use case in factory automation, the sampling period of the sensor is set to $T = 0.02$ s, and the number of information bits at the sensor and controller are set to $l_{\text{u}} = 240$ and $l_{\text{d}} = 160$ with the maximum allowable blocklengths $m_{\text{u,max}} = 400$ c.u. and $m_{\text{d,max}} = 300$ c.u., respectively [10]. Also, the modulation order is set to $\Theta = 16$ and the symbol duration is set to $T_{\text{s}} = 10^{-5}$ s. Both the sensor and controller are allowed to retransmit with the maximum number of allowable transmissions $r = 3$ [17]. The maximum allowable variance and outage probability of PAoL are set to 10 ms and 1%, respectively, with the error tolerance $\xi = 10^{-8}$ in Algorithm 1. The proposed scheme is labeled as 'PAoL-optimal W/ ReTx', and the following designs are selected as benchmarks: 1) UL blocklength optimization for UL PAoI minimization [29] (labeled as 'UL PAoI-optimal [29]'); 2) DL blocklength optimization for DL PAoI minimization [21] (labeled as 'DL PAoI-optimal [21]'); 3) joint optimization of UL and DL blocklengths for PAoL minimization without retransmission (labeled as 'PAoL-optimal W/O ReTx').

A. Average PAoL Performance

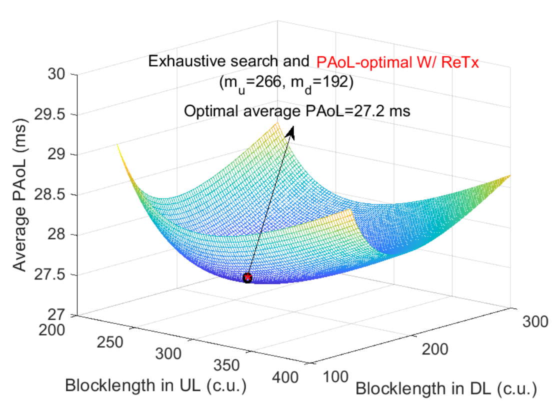

Fig. 3. Joint impact of blocklengths in UL and DL on the average PAoL with sampling period $T = 20$ ms, maximum number of allowable transmissions $r = 3$ and average SNR $\bar{\gamma} = 6$ dB.

Fig. 3 shows the joint impact of blocklengths in UL and DL on the average PAoL with the sampling period $T = 20$ ms, maximum number of allowable transmissions $r = 3$ and the average SNR $\bar{\gamma} = 6$ dB. It is shown that the average PAoL is convex with respect to blocklengths, as proved in Proposition 1. The reason is that with relatively short blocklengths, the BLEPs in UL and DL are high and hence a large interarrival time is obtained, which dominates the average PAoL. While with larger blocklengths, the service time increases and then the average PAoL is larger. Also, it is observed that there exists an optimal blocklength pair that minimizes the average PAoL, and that the proposed PAoL-optimal scheme finds the optimal blocklengths accurately at much lower complexity compared with exhaustive search.

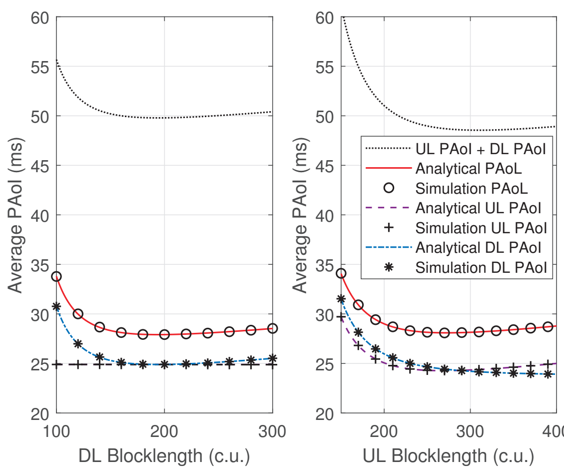

Fig. 4. Impact of the DL (UL) blocklength with the fixed UL (DL) blocklength $m_{\mathrm{u}} = 200$ c.u. ($m_{\mathrm{d}} = 140$ c.u.) on the information freshness of WNCSs, with the sampling period $T = 20$ ms, maximum number of allowable transmissions $r = 3$ and average SNR $\bar{\gamma} = 6$ dB.

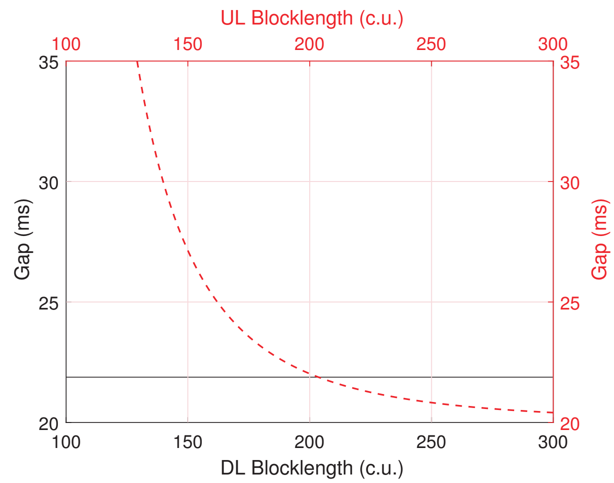

Fig. 5. Impact of DL and UL blocklengths on the gap between the average PAoL and the sum of UL PAoI and DL PAoI, with the sampling period $T = 20$ ms, maximum number of allowable transmissions $r = 3$ and average SNR $\bar{\gamma} = 6$ dB.

Fig. 4 shows the impact of the DL (UL) blocklength with the fixed UL (DL) blocklength on the average PAoL, UL PAoI and DL PAoI, respectively. With the fixed UL blocklength $m_{\mathrm{u}} = 200$ c.u., both the average PAoL and DL PAoI are convex with respect to the DL blocklength, while the average UL PAoI is independent of it, as analyzed in Theorem 1. In contrast, it is shown that the UL blocklength affects the average UL PAoI, DL PAoI and PAoL significantly, as the controller is event-triggered. Also, the average DL PAoI is monotonically decreasing with the UL blocklength , as stated in Corollary 2. This is due to that a larger UL blocklength leads to a lower BLEP and a smaller interarrival time at the controller, which leads to a lower average DL

PAoI. Particularly, Fig. 5 shows that the gap is independent of DL blocklength and decreasing with respect to the UL blocklength. Due to the existence of the gap, the average PAoL is not the sum of the average UL PAoI and DL PAoI, as shown in Fig. 4 and stated in Theorem 2.

B. Variance and outage probability of PAoL Performances

In Fig. 6, impact of the maximum number of allowable transmissions and transmission rate on the standard deviation of PAoL is shown, where the blocklengths in UL and DL are adapted based on different rates. It is shown that with the increase of transmission rate, the variance of PAoL is increasing monotonically, as a higher transmission rate leads to a higher BLEP and impairs the stability of status updating in WNCSs. Also, we can observe that retransmission is beneficial for improving stability and that the standard deviation of PAoL can be reduced significantly with one retransmission. This is due to that with retransmission, the probability of packets being received successfully is improved, which may induce larger service times but a smaller interarrival time. Since the interarrival time is based on the sampling period, which is assumed to be larger than service time, retransmission is able to reduce the variance of PAoL.

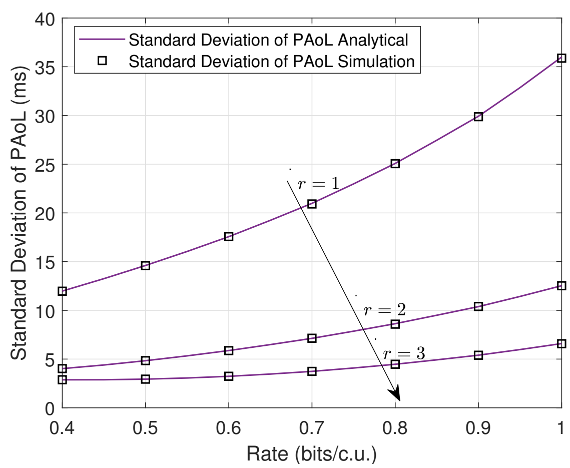

Fig. 6. Impact of the maximum number of allowable transmissions and transmission rate on the standard deviation of PAoL with the sampling period $T = 20$ ms and average SNR $\bar{\gamma} = 6$ dB.

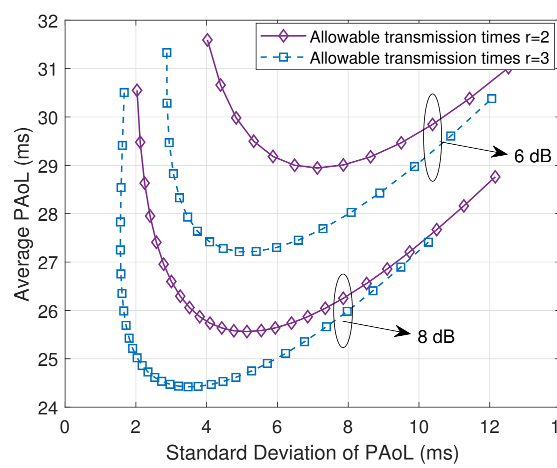

Fig. 7. Impact of the maximum number of allowable transmissions on the relationship between the average PAoL and the standard deviation of PAoL with the adaptation of transmission rate from 0.4 to 1.

In Fig. 7, the relationship between the average PAoL and the standard deviation of PAoL with different numbers of allowable transmissions and transmission rates is shown under average SNR $\bar{\gamma} = 6$ dB and $\bar{\gamma} = 8$ dB. It is observed that there is a tradeoff between the average PAoL and the standard deviation of PAoL with the adaptation of transmission rate and that allowing more transmissions and higher SNRs lead to better average-variance PAoL performances. This implies that minimizing the standard deviation of PAoL may result in a larger average PAoL with low transmission rates, demonstrating the necessity of introducing the variance of PAoL.

In Fig. 8, the impact of the maximum number of allowable transmissions and PAoL threshold on the outage probability of PAoL is shown. The PAoL outage probability is decreasing with respect to the PAoL threshold and the decreasing rate is exponential, as proved in corollary 5. In addition, with a larger number of allowable transmission times, the PAoL outage probability is lower, as stated in Proposition 3. This is due to that allowing more transmissions is able to reduce the interarrival time. Hence, the probability of the worst case of PAoL is lower.

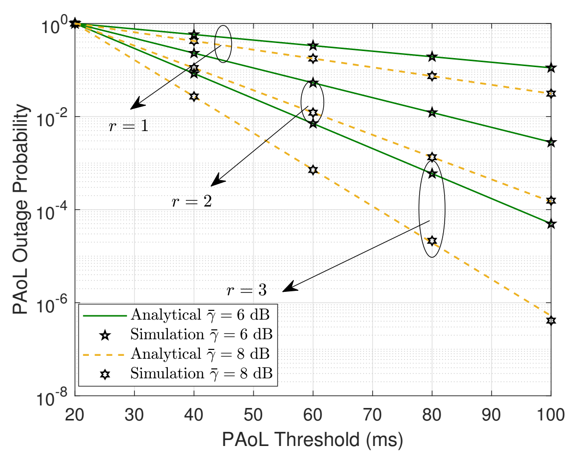

Fig. 8. Impact of the maximum number of allowable transmissions and PAoL threshold on the PAoL outage probability with the fixed blocklengths $m_{\mathrm{u}} = 240$ c.u. and $m_{\mathrm{d}} = 160$ c.u. under average SNR $\bar{\gamma} = 6$ and 8 dB.

C. PAoL-oriented Scheme

In Fig. 9, the optimized average PAoL and its standard deviation obtained by different policies are shown, where the fixed blocklength $m_{\mathrm{d}} = 100$ c.u. in DL is employed in UL PAoI-oriented scheme [29] and the fixed blocklength $m_{\mathrm{u}} = 150$ c.u. in UL is employed in DL PAoI-oriented scheme [21]. It is shown that the PAoL-optimal result achieves the lowest average PAoL and variance of PAoL, compared to the UL PAoI-optimal, DL PAoI-optimal and PAoL-optimal without retransmission results. In Fig. 10, the control performances obtained by different policies are compared in terms of the average control cost and the standard deviation of control cost. The proposed PAoL-oriented scheme can significantly reduce the control cost, especially at low SNR, thanks to a higher degree of freedom on optimization and the consideration of the coupling between UL and DL. This demonstrates that the proposed PAoL-oriented scheme is able to maintain the best PAoL and control performances in the WNCS.

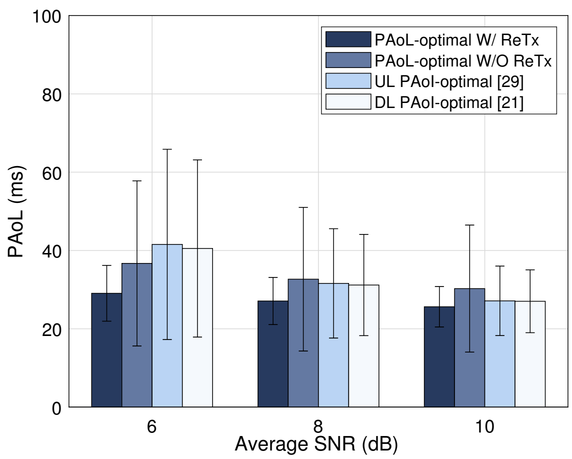

Fig. 9. Optimized average PAoL and standard deviation of PAoL vs. average SNR.

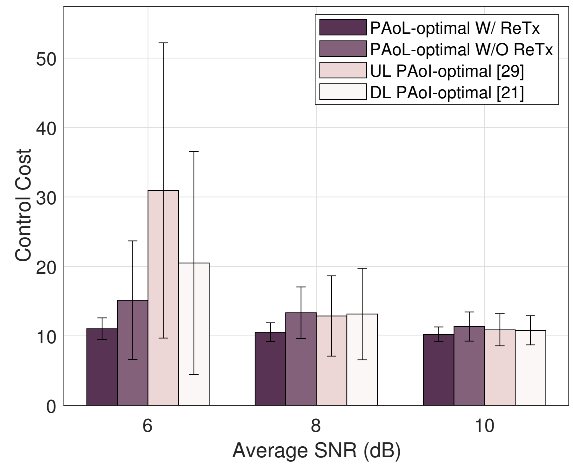

Fig. 10. Optimized average control cost and standard deviation of control cost vs. average SNR.

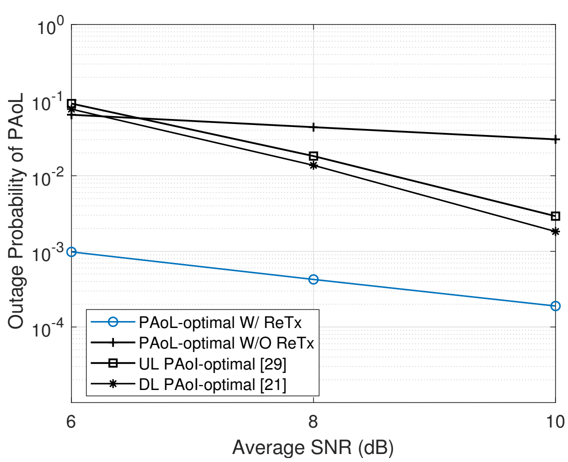

Fig. 11. Optimized outage probability of PAoL vs. average SNR with the PAoL threshold $\delta = 80$ ms.

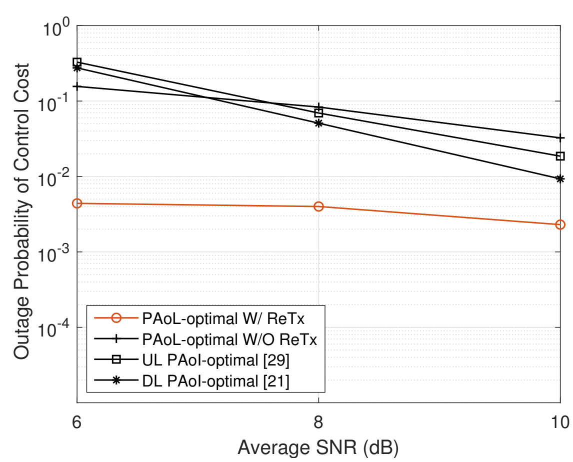

Fig. 12. Optimized outage probability of control cost vs. average SNR with the control cost threshold $\delta_{\text{c}} = 15$.

In Figs. 11 and 12, the optimized outage probability of PAoL and control cost are shown to indicate the extreme-case performance of WNCSs. The outage probability of control cost is obtained by simulations and defined as the probability that the control cost exceeds the given control cost threshold [43], *i.e.*, $\Pr[J > \delta_{\text{c}}] = \lim_{i\to\infty} \Pr[J_i > \delta_{\text{c}}]$, where J_i denotes the control cost of the i-th control round. It is shown that the PAoL-optimal result outperforms the existing schemes in terms of the outage probability of PAoL and control cost. Particulalry, the PAoL-optimal result achieves up to 100-fold PAoL outage probability performance and 80-fold control cost outage probability performance improvements at 6 dB, compared to the UL PAoI-optimal scheme.

In Fig. 13, we show the impact of average SNR on different transmission policies in terms of the average PAoL and the normalized control performance, where the control performance is defined as the reciprocal of the average control cost, *i.e.*, $\frac{1}{J}$, and normalized by the control performance obtained by the PAoL-optimal scheme at 15 dB. Generally, with a higher SNR, the average PAoL is lower and the control performance is better, indicating that a higher average PAoL performance reflects a better control performance. Also, it is shown that the PAoL-optimal scheme achieves the lowest average PAoL and the best control performance, which outperforms the approach without retransmission. Furthermore, the proposed PAoL-optimal scheme outperforms the approach that optimizes UL PAoI or DL PAoI solely, where the improvements of the average PAoL performance and control performance are up to 1.7-fold and 8-fold, respectively, demonstrating that minimizing UL PAoI and DL PAoI is not equivalent to minimizing PAoL and verifying the advantages of the introduced average PAoL.

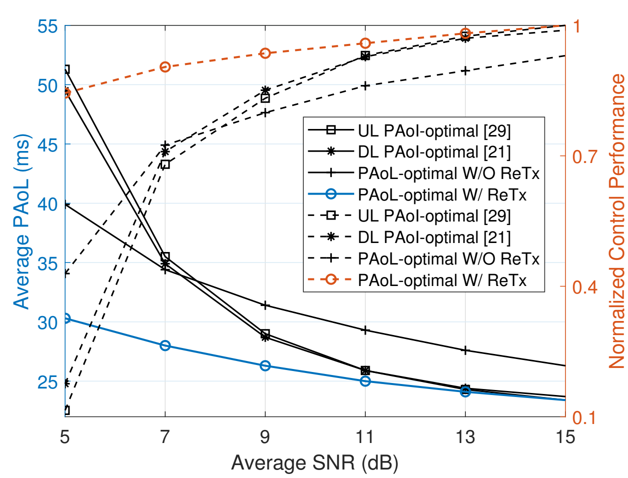

Fig. 13. Optimized average PAoL and the normalized control performance vs. average SNR with different schemes.

VII. Conclusion

In this paper, we have presented a comprehensive analysis on the average, variance and outage PAoL performances of WNCSs with FBL over fading channels, and investigated the co-design of communication and control. The closed-form expressions for the average UL PAoI, DL PAoI and PAoL with respect to blocklengths and maximum number of allowable transmissions have been derived. Based on these, it is proved that the average PAoL is less than the sum of UL PAoI and DL PAoI. In addition, the variance and outage probability of PAoL have been derived in closed forms and have demonstrated the same trend. The accuracy of the theoretical analysis has been confirmed by simulations. Particularly, the PAoL-oriented communication and control co-design has been investigated. An effective PAoL-oriented blocklength adaptation with retransmission scheme has been proposed to minimize the average PAoL subject to the variance and outage probability of PAoL. The optimized maximum number of allowable transmissions and blocklengths are used in the control design. The proposed PAoL-oriented scheme with optimal control has provided better average, variance and outage performances in PAoL and control, compared to the approach that optimizes UL PAoI or DL PAoI solely. In particular, with the proposed PAoL-oriented scheme, the average PAoL is reduced by up to 1.7-fold and the average control cost is improved by up to 8-fold, In addition, the proposed algorithm also results in better extreme-case performance, with up to 80-fold reduction in outage probability of control.

APPENDIX A
PROOF OF THEOREM 1

Based on (8), the average PAoL depends on the average interarrival time $\mathbb{E}[Y^{\mathrm{L}}]$ and service time $\mathbb{E}[S^{\mathrm{L}}]$, which are derived in the following. First, the transmission delay of each round in UL and DL are given by $m_{\mathrm{u}}T_{\mathrm{s}}$ and $m_{\mathrm{d}}T_{\mathrm{s}}$, respectively. Then, with the TARQ policy and maximum number of allowable transmissions r, the average service time in the case of successful transmission is derived as $\mathbb{E}[S^{\mathrm{L}}] = \frac{\sum_{k=1}^{r} k\bar{\epsilon}_{\mathrm{u}}^{k-1}(1-\bar{\epsilon}_{\mathrm{u}})m_{\mathrm{u}}T_{\mathrm{s}}}{1-\bar{\epsilon}_{\mathrm{u}}^{r}} + \frac{\sum_{k=1}^{r} k\bar{\epsilon}_{\mathrm{d}}^{k-1}(1-\bar{\epsilon}_{\mathrm{d}})m_{\mathrm{d}}T_{\mathrm{s}}}{1-\bar{\epsilon}_{\mathrm{d}}^{r}}$. This can be obtained based on the fact that PAoL characterizes the timeliness of packets generated from the sensor and received by the actuator, and that the service times in UL and DL are independent. Based on the series expansion $\sum_{k=1}^{r} kx^{k-1} = \frac{rx^{r+1}-rx^{r}-x^{r}+1}{(1-x)^2}$ [35], we have $\mathbb{E}[S^{\mathrm{L}}] = \frac{m_{\mathrm{u}}T_{\mathrm{s}}}{1-\bar{\epsilon}_{\mathrm{u}}} - \frac{r\bar{\epsilon}_{\mathrm{u}}^{r}m_{\mathrm{u}}T_{\mathrm{s}}}{1-\bar{\epsilon}_{\mathrm{u}}^{r}} + \frac{m_{\mathrm{d}}T_{\mathrm{s}}}{1-\bar{\epsilon}_{\mathrm{d}}} - \frac{r\bar{\epsilon}_{\mathrm{d}}^{r}m_{\mathrm{d}}T_{\mathrm{s}}}{1-\bar{\epsilon}_{\mathrm{d}}^{r}}$, as shown in (9). Then, based on the fact that instantaneous AoL drops only when both packets in UL and DL are transmitted successfully, the interarrival time can be derived as follows. Considering the BLEP $\bar{\epsilon}_{\mathrm{u}}$ in UL and $\bar{\epsilon}_{\mathrm{d}}$ in DL, and letting $\chi = 1-(1-\bar{\epsilon}_{\mathrm{u}}^{r})(1-\bar{\epsilon}_{\mathrm{d}}^{r})$ denote the probability of unsuccessful transmission for both UL and DL, the average interarrival time of informative packets is given as $\mathbb{E}[Y^{\mathrm{L}}] = \sum_{k=0}^{\infty}(k+1)\chi^{k}T(1-\chi)$. This is due to that the interarrival time increases a sampling period T when the transmission error occurs in UL or DL. Applying the series expansions $\sum_{k=0}^{\infty} x^k = \frac{1}{1-x}$ and $\sum_{k=0}^{\infty} kx^k = \frac{x}{(1-x)^2}$, we have $\mathbb{E}[Y^{\mathrm{L}}] = \frac{T}{(1-\bar{\epsilon}_{\mathrm{u}}^r)(1-\bar{\epsilon}_{\mathrm{d}}^r)}$, as provided in (10). Hence, the average PAoL in (11) can be derived and (12) is obtained by letting $r=1$. In addition, the first-order derivative of the average PAoL with respect to r is given by $\frac{\partial \bar{A}^{\mathrm{L}}}{\partial r} = \frac{T\bar{\epsilon}_{\mathrm{u}}^r \ln(\bar{\epsilon}_{\mathrm{u}}) - m_{\mathrm{u}} T_{\mathrm{s}} \bar{\epsilon}_{\mathrm{u}}^r (\ln(\bar{\epsilon}_{\mathrm{u}}) r - \bar{\epsilon}_{\mathrm{u}}^r + 1)(1-\bar{\epsilon}_{\mathrm{d}}^r)}{(1-\bar{\epsilon}_{\mathrm{d}}^r)(1-\bar{\epsilon}_{\mathrm{u}}^r)^2} + \frac{T\bar{\epsilon}_{\mathrm{d}}^r \ln(\bar{\epsilon}_{\mathrm{d}}) - m_{\mathrm{d}} \bar{\epsilon}_{\mathrm{d}}^r (\ln(\bar{\epsilon}_{\mathrm{d}}) r - \bar{\epsilon}_{\mathrm{d}}^r + 1)(1-\bar{\epsilon}_{\mathrm{u}}^r)}{(1-\bar{\epsilon}_{\mathrm{d}}^r)^2(1-\bar{\epsilon}_{\mathrm{u}}^r)}$. Since $0 < \bar{\epsilon}_{\mathrm{u}} < 1$ and $0 < \bar{\epsilon}_{\mathrm{d}} < 1$, $\ln(\bar{\epsilon}_{\mathrm{u}}) < 0$ and $\ln(\bar{\epsilon}_{\mathrm{d}}) < 0$ holds. Based on the assumption of $T > r(m_{\mathrm{u}} + m_{\mathrm{d}})T_{\mathrm{s}}$ provided in Subsection II-B, $\frac{\partial \bar{A}^{\mathrm{L}}}{\partial r} < 0$ is guaranteed.

Appendix B
Proof of Corollary 2

We aim to prove that minimizing the average PAoL is not equivalent to minimizing the sum of UL PAoI and DL PAoI. Based on (13), the first-order derivative of the average PAoL with respect to the blocklength in UL is given as $\frac{\partial \bar{A}^{\mathrm{L}}}{\partial m_{\mathrm{u}}} = \frac{\partial (\bar{A}^{\mathrm{U}} + \bar{A}^{\mathrm{D}})}{\partial m_{\mathrm{u}}} - \frac{T}{(1-\bar{\epsilon}_{\mathrm{u}}^r)^2} \frac{\partial \bar{\epsilon}_{\mathrm{u}}^r}{\partial m_{\mathrm{u}}}$. Since the term $\frac{T}{(1-\bar{\epsilon}_{\mathrm{u}}^r)^2} \frac{\partial \bar{\epsilon}_{\mathrm{u}}^r}{\partial m_{\mathrm{u}}}$ is not zero with the non-zero term $\frac{\partial \bar{\epsilon}_{\mathrm{u}}^r}{\partial m_{\mathrm{u}}}$, there exist different blocklengths that minimize the average PAoL and the sum of UL PAoI and DL PAoI. In addition, based on (15), the first-order derivative of the average DL PAoI with respect to the blocklength in UL is given by $\frac{\partial \bar{A}^{\mathrm{D}}}{\partial m_{\mathrm{u}}} = \frac{T \frac{\partial \bar{\epsilon}_{\mathrm{u}}^r}{m_{\mathrm{u}}}}{(1-\bar{\epsilon}_{\mathrm{u}}^r)^2(1-\bar{\epsilon}_{\mathrm{d}}^r)}$. Based on the average BLEP in (3), we have $\frac{\partial \bar{A}^{\mathrm{D}}}{\partial m_{\mathrm{u}}} = \frac{T(\sqrt{\pi l_{\mathrm{u}}} - l_{\mathrm{u}} e^{\frac{l_{\mathrm{u}}}{m_{\mathrm{u}}}})}{(1-\bar{\epsilon}_{\mathrm{u}}^r)^2(1-\bar{\epsilon}_{\mathrm{d}}^r)\bar{\gamma} m_{\mathrm{u}}^2} e^{\frac{-e^{\frac{l_{\mathrm{u}}}{m_{\mathrm{u}}}} + \frac{\sqrt{\pi l_{\mathrm{u}}}}{m_{\mathrm{u}}} + 1}{\bar{\gamma}}}$. As $e^{\frac{l_{\mathrm{u}}}{m_{\mathrm{u}}}} > 1$, $\frac{\partial \bar{A}^{\mathrm{D}}}{\partial m_{\mathrm{u}}} < 0$ is held when $l_{\mathrm{u}} \geq \pi$, which is easy to be satisfied in typical real-time applications [21]. Hence, the average DL PAoI is monotonically decreasing with respect to the blocklength m_{u} in UL if $l_{\mathrm{u}} \geq \pi$.

Appendix C
Proof of Theorem 3

Due to the independence of interarrival time and service time, we have $\mathrm{Var}[A^{\mathrm{L}}] = \mathrm{Var}[Y^{\mathrm{L}}] + \mathrm{Var}[S^{\mathrm{L}}]$, which can be further expressed as $\mathrm{Var}[A^{\mathrm{L}}] = \mathrm{Var}[Y^{\mathrm{L}}] + \mathrm{Var}[S_{\mathrm{u}}] + \mathrm{Var}[S_{\mathrm{d}}]$, as the service times in UL and DL are independent. The expectation of the second moment of interarrival time is given by $\mathbb{E}[Y^{\mathrm{L}^2}] = \sum_{k=0}^{\infty}(k+1)^2 T^2 (1-\chi)\chi^k = \frac{1+\chi}{(1-\chi)^2} T^2$ based on the series expansion. Also, we have $\mathbb{E}[Y^{\mathrm{L}}]^2 = \frac{1}{(1-\chi)^2} T^2$ based on (10). Hence, $\mathrm{Var}[Y^{\mathrm{L}}] = \mathbb{E}[Y^{\mathrm{L}^2}] - \mathbb{E}[Y^{\mathrm{L}}]^2 = \frac{\chi}{(1-\chi)^2} T^2$ can be obtained. For the service time in UL, $\mathbb{E}[S_{\mathrm{u}}^2] = \frac{\sum_{k=1}^{r} \bar{\epsilon}_{\mathrm{u}}^{k-1}(1-\bar{\epsilon}_{\mathrm{u}}) k^2 m_{\mathrm{u}}^2 T_{\mathrm{s}}^2}{1-\bar{\epsilon}_{\mathrm{u}}^r} = \frac{-r^2 \bar{\epsilon}_{\mathrm{u}}^r}{1-\bar{\epsilon}_{\mathrm{u}}^r} - \frac{2r\bar{\epsilon}_{\mathrm{u}}^r}{(1-\bar{\epsilon}_{\mathrm{u}})(1-\bar{\epsilon}_{\mathrm{u}}^r)} + \frac{1+\bar{\epsilon}_{\mathrm{u}}}{(1-\bar{\epsilon}_{\mathrm{u}})^2}$ is derived. In addition, $\mathbb{E}[S_{\mathrm{u}}]^2 = \frac{m_{\mathrm{u}}^2 T_{\mathrm{s}}^2}{(1-\bar{\epsilon}_{\mathrm{u}})^2} + \frac{m_{\mathrm{u}}^2 T_{\mathrm{s}}^2 r^2 \bar{\epsilon}_{\mathrm{u}}^{2r}}{(1-\bar{\epsilon}_{\mathrm{u}}^r)^2} - \frac{2m_{\mathrm{u}}^2 T_{\mathrm{s}}^2 r \bar{\epsilon}_{\mathrm{u}}^r}{(1-\bar{\epsilon}_{\mathrm{u}})(1-\bar{\epsilon}_{\mathrm{u}}^r)}$ is derived based on (9). Then we have $\mathrm{Var}[S_{\mathrm{u}}] = \mathbb{E}[S_{\mathrm{u}}^2] - \mathbb{E}[S_{\mathrm{u}}]^2 = \frac{m_{\mathrm{u}}^2 T_{\mathrm{s}}^2 \bar{\epsilon}_{\mathrm{u}}}{(1-\bar{\epsilon}_{\mathrm{u}})^2} - \frac{m_{\mathrm{u}}^2 T_{\mathrm{s}}^2 r^2 \bar{\epsilon}_{\mathrm{u}}^r}{(1-\bar{\epsilon}_{\mathrm{u}}^r)^2}$. Similarly, we have $\mathrm{Var}[S_{\mathrm{d}}] = \mathbb{E}[S_{\mathrm{d}}^2] - \mathbb{E}[S_{\mathrm{d}}]^2 = \frac{m_{\mathrm{d}}^2 T_{\mathrm{s}}^2 \bar{\epsilon}_{\mathrm{d}}}{(1-\bar{\epsilon}_{\mathrm{d}})^2} - \frac{m_{\mathrm{d}}^2 T_{\mathrm{s}}^2 r^2 \bar{\epsilon}_{\mathrm{d}}^r}{(1-\bar{\epsilon}_{\mathrm{d}}^r)^2}$. Therefore, substituting the derived $\mathrm{Var}[Y^{\mathrm{L}}]$, $\mathrm{Var}[S_{\mathrm{u}}]$ and $\mathrm{Var}[S_{\mathrm{d}}]$ into $\mathrm{Var}[A^{\mathrm{L}}] = \mathrm{Var}[Y^{\mathrm{L}}] + \mathrm{Var}[S_{\mathrm{u}}] + \mathrm{Var}[S_{\mathrm{d}}]$ yields the variance of PAoL in (18). By letting $r = 1$,

(18) reduces to (19). Then we prove the monotonicity of the variance of PAoL with respect to the maximum number of allowable transmissions, *i.e.*, $\frac{\partial \mathrm{Var}[A^{\mathrm{L}}]}{\partial r} < 0$, by proving $\frac{\partial F}{\partial r} < 0$, where $F = \frac{T^2(\bar{\epsilon}_{\mathrm{u}}^r + \bar{\epsilon}_{\mathrm{d}}^r - \bar{\epsilon}_{\mathrm{u}}^r \bar{\epsilon}_{\mathrm{d}}^r)}{(1-\bar{\epsilon}_{\mathrm{u}}^r)^2(1-\bar{\epsilon}_{\mathrm{d}}^r)^2} - \frac{m_{\mathrm{u}}^2 T_{\mathrm{s}}^2 r^2 \bar{\epsilon}_{\mathrm{u}}^r}{(1-\bar{\epsilon}_{\mathrm{u}}^r)^2} - \frac{m_{\mathrm{d}}^2 T_{\mathrm{s}}^2 r^2 \bar{\epsilon}_{\mathrm{d}}^r}{(1-\bar{\epsilon}_{\mathrm{d}}^r)^2} = \frac{T^2 \bar{\epsilon}_{\mathrm{u}}^r/(1-\bar{\epsilon}_{\mathrm{d}}^r) - m_{\mathrm{u}}^2 T_{\mathrm{s}}^2 r^2 \bar{\epsilon}_{\mathrm{u}}^r}{(1-\bar{\epsilon}_{\mathrm{u}}^r)^2} + \frac{T^2 \bar{\epsilon}_{\mathrm{d}}^r/(1-\bar{\epsilon}_{\mathrm{u}}^r)^2 - m_{\mathrm{d}}^2 T_{\mathrm{s}}^2 r^2 \bar{\epsilon}_{\mathrm{d}}^r}{(1-\bar{\epsilon}_{\mathrm{d}}^r)^2}$. Since the average BLEPs are smaller than 1, *i.e.*, $0 < \bar{\epsilon}_{\mathrm{u}} < 1$ and $0 < \bar{\epsilon}_{\mathrm{d}} < 1$, $1 - \bar{\epsilon}_{\mathrm{u}}^r$ and $1 - \bar{\epsilon}_{\mathrm{d}}^r$ are positive and increasing with respect to the maximum number of allowable transmissions r. Therefore, we prove that $F_1 > 0$, $\frac{\partial F_1}{\partial r} < 0$, $F_2 > 0$ and $\frac{\partial F_2}{\partial r} < 0$ in the following, where $F_1 = T^2 \bar{\epsilon}_{\mathrm{u}}^r/(1-\bar{\epsilon}_{\mathrm{d}}^r) - m_{\mathrm{u}}^2 T_{\mathrm{s}}^2 r^2 \bar{\epsilon}_{\mathrm{u}}^r$ and $F_2 = T^2 \bar{\epsilon}_{\mathrm{d}}^r/(1-\bar{\epsilon}_{\mathrm{u}}^r)^2 - m_{\mathrm{d}}^2 T_{\mathrm{s}}^2 r^2 \bar{\epsilon}_{\mathrm{d}}^r$. First, $F_1 > 0$ is held as $T^2 > m_{\mathrm{u}}^2 T_{\mathrm{s}}^2 r^2$. Also, we have $\frac{\partial F_1}{\partial r} = \frac{T^2 \ln(\bar{\epsilon}_{\mathrm{u}}) \bar{\epsilon}_{\mathrm{u}}^r}{1-\bar{\epsilon}_{\mathrm{d}}^r} - m_{\mathrm{u}}^2 T_{\mathrm{s}}^2 r^2 \ln(\bar{\epsilon}_{\mathrm{u}}) \bar{\epsilon}_{\mathrm{u}}^r - 2 m_{\mathrm{u}}^2 T_{\mathrm{s}}^2 r \bar{\epsilon}_{\mathrm{d}}^r + \frac{T^2 \ln(\bar{\epsilon}_{\mathrm{d}}) \bar{\epsilon}_{\mathrm{u}}^r \bar{\epsilon}_{\mathrm{d}}^r}{(1-\bar{\epsilon}_{\mathrm{d}}^r)^2}$. As $\ln(\bar{\epsilon}_{\mathrm{u}}) < 0$ and $\ln(\bar{\epsilon}_{\mathrm{d}}) < 0$, $\frac{\partial F_1}{\partial r} < 0$ is proved. Then, $F_2 > 0$ and $\frac{\partial F_2}{\partial r} < 0$ can be proved in a similar way. Hence, $\frac{\partial \mathrm{Var}[A^{\mathrm{L}}]}{\partial r} < 0$ is proved.

APPENDIX D
PROOF OF THEOREM 4

As stated in (11), the average PAoL consists of the interarrival time Y^{L} and service time in UL S_{u} and DL S_{d}, which are independent with each other. Then, the transmission delay with block lengths $(m_{\mathrm{u}}, m_{\mathrm{d}})$ and number of transmission times $(r_{\mathrm{u}}, r_{\mathrm{d}})$ is obtained as $r_{\mathrm{u}} m_{\mathrm{u}} T_{\mathrm{s}} + r_{\mathrm{d}} m_{\mathrm{d}} T_{\mathrm{s}}$ with the probability of $(1-\bar{\epsilon}_{\mathrm{u}})(1-\bar{\epsilon}_{\mathrm{d}}) \bar{\epsilon}_{\mathrm{u}}^{r_{\mathrm{u}}-1} \bar{\epsilon}_{\mathrm{d}}^{r_{\mathrm{d}}-1}$. Since PAoL A^{L} is larger than δ when the transmission round is larger than $\frac{\delta - r_{\mathrm{u}} m_{\mathrm{u}} T_{\mathrm{s}} - r_{\mathrm{d}} m_{\mathrm{d}} T_{\mathrm{s}}}{T}$, the minimum transmission round is given as $\phi = \lceil \frac{\delta - r_{\mathrm{u}} m_{\mathrm{u}} T_{\mathrm{s}} - r_{\mathrm{d}} m_{\mathrm{d}} T_{\mathrm{s}}}{T} \rceil$, with the probability of $(1-(1-\bar{\epsilon}_{\mathrm{u}}^r)(1-\bar{\epsilon}_{\mathrm{d}}^r))^{\phi}(1-\bar{\epsilon}_{\mathrm{u}}^r)(1-\bar{\epsilon}_{\mathrm{d}}^r)$. With the number of allowable transmissions r, the PAoL outage probability is given by $\Pr[A^{\mathrm{L}} > \delta] = \frac{1}{1-\chi} \sum_{r_{\mathrm{u}}=1}^{r} \sum_{r_{\mathrm{d}}=1}^{r} \sum_{i=\phi}^{\infty} (1-(1-\bar{\epsilon}_{\mathrm{u}}^r)(1-\bar{\epsilon}_{\mathrm{d}}^r))^{i-1}(1-\bar{\epsilon}_{\mathrm{u}}^r)(1-\bar{\epsilon}_{\mathrm{d}}^r)(1-\bar{\epsilon}_{\mathrm{u}})(1-\bar{\epsilon}_{\mathrm{d}}) \bar{\epsilon}_{\mathrm{u}}^{r_{\mathrm{u}}-1} \bar{\epsilon}_{\mathrm{d}}^{r_{\mathrm{d}}-1}$. Based on the series expansion $\sum_{i=\phi}^{\infty} \chi^{i-1}(1-\chi) = \chi^{\phi-1}$, we have $\Pr[A^{\mathrm{L}} > \delta] = \sum_{r_{\mathrm{u}}=1}^{r} \sum_{r_{\mathrm{d}}=1}^{r} \frac{\chi^{\phi-1}}{1-\chi}(1-\bar{\epsilon}_{\mathrm{u}})(1-\bar{\epsilon}_{\mathrm{d}}) \bar{\epsilon}_{\mathrm{u}}^{r_{\mathrm{u}}-1} \bar{\epsilon}_{\mathrm{d}}^{r_{\mathrm{d}}-1}$. As $r_{\mathrm{u}} m_{\mathrm{u}} T_{\mathrm{s}} + r_{\mathrm{d}} m_{\mathrm{d}} T_{\mathrm{s}} < T$ is held, $\frac{r_{\mathrm{u}} m_{\mathrm{u}} T_{\mathrm{s}} + r_{\mathrm{d}} m_{\mathrm{d}} T_{\mathrm{s}}}{T} < 1$ is guaranteed. Also, the first-order derivative of the PAoL outage probability with respect to r is given as $\frac{\partial \Pr[A^{\mathrm{L}} > \delta]}{\partial r} = (\frac{\delta}{T} - 1)(\chi)^{\frac{\delta}{T}-2} (\ln(\bar{\epsilon}_{\mathrm{d}})(1-\bar{\epsilon}_{\mathrm{u}}^r)\bar{\epsilon}_{\mathrm{d}}^r + \ln(\bar{\epsilon}_{\mathrm{u}})(1-\bar{\epsilon}_{\mathrm{d}}^r)\bar{\epsilon}_{\mathrm{u}}^r)$. Since $0 < \bar{\epsilon}_{\mathrm{u}} < 1$ and $0 < \bar{\epsilon}_{\mathrm{d}} < 1$, we have $\ln(\bar{\epsilon}_{\mathrm{u}}) < 0$ and $\ln(\bar{\epsilon}_{\mathrm{d}}) < 0$. Therefore, $\frac{\partial \Pr[A^{\mathrm{L}} > \delta]}{\partial r} < 0$ is guaranteed when $\delta > T$.

APPENDIX E
PROOF OF PROPOSITION 1

In this appendix, we prove the convexity of the average PAoL based on the second-order derivative of the average PAoL with respect to the blocklength. Regarding the UL, we have $\frac{\partial^2 \bar{A}^{\mathrm{L}}}{\partial {m_{\mathrm{u}}}^2} = Z_1 + Z_2 + Z_3$, where $Z_1 = \frac{\frac{T}{1-\bar{\epsilon}_{\mathrm{d}}^r} \frac{\partial^2 \bar{\epsilon}_{\mathrm{u}}^r}{\partial {m_{\mathrm{u}}}^2}(1-\bar{\epsilon}_{\mathrm{u}}^r) + \frac{2T}{1-\bar{\epsilon}_{\mathrm{d}}^r}(\frac{\partial \bar{\epsilon}_{\mathrm{u}}^r}{\partial m_{\mathrm{u}}})^2}{(1-\bar{\epsilon}_{\mathrm{u}}^r)^3}$, $Z_2 = \frac{m_{\mathrm{u}} T_{\mathrm{s}} \frac{\partial^2 \bar{\epsilon}_{\mathrm{u}}}{\partial m_{\mathrm{u}}^2}(1-\bar{\epsilon}_{\mathrm{u}}) + 2T_{\mathrm{s}}(1-\bar{\epsilon}_{\mathrm{u}})\frac{\partial \bar{\epsilon}_{\mathrm{u}}}{\partial m_{\mathrm{u}}} + 2 m_{\mathrm{u}} T_{\mathrm{s}} (\frac{\partial \bar{\epsilon}_{\mathrm{u}}}{\partial m_{\mathrm{u}}})^2}{(1-\bar{\epsilon}_{\mathrm{u}})^3}$ and

$Z_3 = \frac{m_{\rm u}T_{\rm s}r\frac{\partial^2 \bar{\epsilon}_{\rm u}^r}{\partial m_{\rm u}^2}(1-\bar{\epsilon}_{\rm u}^r)+2T_{\rm s}r(1-\bar{\epsilon}_{\rm u}^r)\frac{\partial \bar{\epsilon}_{\rm u}^r}{\partial m_{\rm u}}+2m_{\rm u}T_{\rm s}r(\frac{\partial \bar{\epsilon}_{\rm u}^r}{\partial m_{\rm u}})^2}{(1-\bar{\epsilon}_{\rm u}^r)^3}$. Based on their numerators, we introduce auxiliary variables $Z_4 = (\frac{2T}{1-\bar{\epsilon}_{\rm d}^r} - 2mT_{\rm s}r)(\frac{\partial \bar{\epsilon}_{\rm u}^r}{\partial m_{\rm u}})^2 + 2m_{\rm u}T_{\rm s}(\frac{\partial \bar{\epsilon}_{\rm u}}{\partial m_{\rm u}})^2$, $Z_5 = (\frac{T}{1-\bar{\epsilon}_{\rm d}^r} - m_{\rm u}T_s r)\frac{\partial \bar{\epsilon}_{\rm u}^r}{\partial m_{\rm u}^2} + m_{\rm u}T_{\rm s}\frac{\partial^2 \bar{\epsilon}_{\rm u}}{\partial m_{\rm u}^2}$ and $Z_6 = -2T_{\rm s}r(1-\bar{\epsilon}_{\rm u}^r)\frac{\partial \bar{\epsilon}_{\rm u}^r}{\partial m_{\rm u}} + 2T_{\rm s}(1-\bar{\epsilon}_{\rm u})\frac{\partial \bar{\epsilon}_{\rm u}}{\partial m_{\rm u}}$. Since $0 < \bar{\epsilon}_{\rm u} < 1$, $Z_1 + Z_2 + Z_3 > 0$ is guaranteed by proving $Z_4 + Z_5 + Z_6 > 0$. First, since $\frac{T}{1-\bar{\epsilon}_{\rm d}^r} - m_{\rm u}T_s r > 0$ is held, $Z_4 > 0$ is proved. Then, we have $Z_5 = ((\frac{T}{1-\bar{\epsilon}_{\rm d}^r} - m_{\rm u}T_s r)r! + m_{\rm u}T_{\rm s})\frac{\partial^2 \bar{\epsilon}_{\rm u}}{\partial m_{\rm u}^2}$. Also, based on the first-order Taylor approximation of $\bar{\epsilon}_{\rm u}$ [21], we have $\frac{\partial^2 \bar{\epsilon}_{\rm u}}{\partial m_{\rm u}^2} \approx \frac{(2l_{\rm u}m_{\rm u}+l_{\rm u}^2)e^{l_{\rm u}/m_{\rm u}} - 2\sqrt{\pi l_{\rm u}}m_{\rm u}}{m_{\rm u}^4\bar{\gamma}} > 0$ if $l_{\rm u} \geq \pi$, which is easily satisfied for typical scenarios [21]. Then, $Z_6 > 0$ holds as $\frac{\partial \bar{\epsilon}_{\rm u}}{\partial m_{\rm u}} = \frac{(\sqrt{\pi l_{\rm u}} - l_{\rm u}e^{\frac{l_{\rm u}}{m_{\rm u}}})}{\bar{\gamma}m_{\rm u}^2}e^{\frac{-e^{\frac{l_{\rm u}}{m_{\rm u}}}+\frac{\sqrt{\pi l_{\rm u}}}{m_{\rm u}}+1}{\bar{\gamma}}} < 0$. Then, $\frac{\partial^2 \bar{A}^{\rm L}}{\partial m_{\rm d}{}^2} > 0$ can be proved in a similar way. In addition, we have $\frac{\partial \bar{A}^{\rm L}}{\partial m_{\rm u}\partial m_{\rm d}} = \frac{T\frac{\partial \bar{\epsilon}_{\rm u}^r}{\partial m_{\rm u}}\frac{\partial \bar{\epsilon}_{\rm d}^r}{\partial m_{\rm d}}}{(1-\bar{\epsilon}_{\rm d}^r)^2(1-\bar{\epsilon}_{\rm u}^r)^2}$ and $Z_1 = \frac{T\frac{\partial^2 \bar{\epsilon}_{\rm u}^r}{\partial m_{\rm u}{}^2}(1-\bar{\epsilon}_{\rm d}^r)+2T\frac{1-\bar{\epsilon}_{\rm d}^r}{1-\bar{\epsilon}_{\rm u}^r}(\frac{\partial \bar{\epsilon}_{\rm u}^r}{\partial m_{\rm u}})^2}{(1-\bar{\epsilon}_{\rm u}^r)^2(1-\bar{\epsilon}_{\rm d}^r)^2}$. Then, $\frac{\partial^2 \bar{A}^{\rm L}}{\partial m_{\rm u}{}^2}\frac{\partial^2 \bar{A}^{\rm L}}{\partial m_{\rm d}^2} - \frac{\partial \bar{A}^{\rm L}}{\partial m_{\rm u}\partial m_{\rm d}}\frac{\partial \bar{A}^{\rm L}}{\partial m_{\rm d}\partial m_{\rm u}} > 0$ when $\bar{\epsilon}_{\rm d}^r - \bar{\epsilon}_{\rm u}^r < 0.5$, which is true for the typical real-time applications [40]. Hence, the Hessian matrix of the objective function with respect to blocklengths are positive definite.

APPENDIX F
PROOF OF PROPOSITION 2

Without loss of generality, we prove the monotonicity of variance of PAoL with respect to the blocklength based on (19). As the denominator of (19) is monotonically increasing along with the blocklength, we prove that the numerator of (19) is decreasing with respect to the blocklength in the following. Letting $F_3 = \bar{\epsilon}_{\rm u} + \bar{\epsilon}_{\rm d} - \bar{\epsilon}_{\rm u}\bar{\epsilon}_{\rm d}$, we have $\frac{\partial F_3}{\partial m_{\rm u}} = (1-\bar{\epsilon}_{\rm d})\frac{\partial \bar{\epsilon}_{\rm u}}{\partial m_{\rm u}} < 0$ and $\frac{\partial F_3}{\partial m_{\rm d}} = (1-\bar{\epsilon}_{\rm u})\frac{\partial \bar{\epsilon}_{\rm d}}{\partial m_{\rm d}} < 0$. Then, the variance of PAoL is decreasing with respect to the blocklength. The first-order derivative of the PAoL outage probability with respect to the BLEP in UL and DL is given by $\frac{\partial \chi}{\partial \bar{\epsilon}_{\rm u}} = r(1-\bar{\epsilon}_{\rm d}^r)(\bar{\epsilon}_{\rm u}^{r-1}) > 0$ and $\frac{\partial \chi}{\partial \bar{\epsilon}_{\rm d}} = r(1-\bar{\epsilon}_{\rm u}^r)(\bar{\epsilon}_{\rm d}^{r-1}) > 0$, respectively. Since $\frac{\partial \bar{\epsilon}_{\rm u}}{\partial m_{\rm u}} < 0$ and $\frac{\partial \bar{\epsilon}_{\rm d}}{\partial m_{\rm d}} < 0$ hold, $\frac{\partial \Pr[{\rm A^L} > \delta]}{\partial m_{\rm u}} < 0$ and $\frac{\partial \Pr[{\rm A^L} > \delta]}{\partial m_{\rm d}} < 0$ can be proved.

REFERENCES

[1] J. Cao, X. Zhu, S. Sun, P. Popovski, S. Feng and Y. Jiang, "Age of Loop Oriented Wireless Networked Control System: Communication and Control Co-Design in the FBL Regime," in *proc. IEEE Conf. Comput. Commun. (INFOCOM) Workshops*, Virtual, May 2022, pp. 1-6.

[2] M. A. Abd-Elmagid, N. Pappas, and H. S. Dhillon, "On the role of age of information in the Internet of Things," *IEEE Commun. Mag.*, vol. 57, no. 12, pp. 72–77, Dec. 2019.

[3] S. Kaul, R. Yates, and M. Gruteser, "Real-time status: How often should one update?" in *Proc. IEEE Conf. Comput. Commun. (INFOCOM)*, Orlando, FL, USA, Mar. 2012, pp. 2731–2735.

[4] M. Costa, M. Codreanu, and A. Ephremides, "On the age of information in status update systems with packet management," *IEEE Trans. Inf. Theory*, vol. 62, pp. 1897–1910, Apr. 2016.

[5] L. Huang and E. Modiano, “Optimizing age-of-information in a multi-class queueing system,” in *Proc. IEEE Int. Symp. Inf. Theory (ISIT)*, Hong Kong, China, Jun. 2015, pp. 1681–1685.

[6] K. Huang, W. Liu, Y. Li, A. Savkin and B. Vucetic, “Wireless feedback control with variable packet length for industrial IoT,” *IEEE Wireless Commun. Lett.*, vol. 9, no. 9, pp. 1586-1590, Sep. 2020.

[7] Y. Polyanskiy, H. V. Poor, and S. Verdú, “Channel coding rate in the finite blocklength regime,” *IEEE Trans. Inf. Theory*, vol. 56, no. 5, pp. 2307–2359, May 2010.

[8] J. Cao et al., “Independent Pilots vs. Shared Pilot: Short Frame Structure Optimization for Heterogeneous-Traffic URLLC Networks,” *IEEE Trans. Wirel. Commun.*, Early Access 2022.

[9] G. Durisi, T. Koch, and P. Popovski, “Toward massive, ultrareliable, and low-latency wireless communication with short packets,” *Proc. IEEE*, vol. 104, pp. 1711–1726, Sep. 2016.

[10] V. 3GPP, TS 22.104, “Service requirements for cyber-physical control applications in vertical domains; stage-1 (release 17),” Jun. 2019.

[11] C. Kam, S. Kompella, and A. Ephremides, “Age of information under random updates,” in *Proc. IEEE Int. Symp. Inf. Theory (ISIT)*, Istanbul, Turkey, Jul. 2013, pp. 66–70.

[12] C. Kam, S. Kompella, G. D. Nguyen, and A. Ephremides, “Effect of message transmission path diversity on status age,” *IEEE Trans. Inf. Theory*, vol. 62, no. 3, pp. 1360–1374, Mar. 2016.

[13] A. M. Bedewy, Y. Sun, and N. B. Shroff, “Optimizing data freshness, throughput, and delay in multi-server information-update systems,” in *Proc. IEEE Int. Symp. Inf. Theory (ISIT)*, Barcelona, Spain, Jul. 2016, pp. 2569–2573.

[14] M. Moltafet, M. Leinonen, and M. Codreanu, “On the age of information in multi-source queueing models,” *IEEE Trans. Commun.*, vol. 68, no. 8, pp. 5003–5017, Aug. 2020.

[15] G. Stamatakis, N. Pappas and A. Traganitis, “Optimal policies for status update generation in an IoT device with heterogeneous traffic,” *IEEE Internet Things J.*, vol. 7, no. 6, pp. 5315-5328, Jun. 2020.

[16] K. Chen and L. Huang, “Age-of-information in the presence of error,” in *Proc. IEEE Int. Symp. Inf. Theory (ISIT)*, Barcelona, Spain, Jul. 2016, pp. 2579–2583.

[17] Y. Gu, H. Chen, Y. Zhou, Y. Li and B. Vucetic, “Timely status update in internet of things monitoring systems: An age-energy tradeoff,” *IEEE Internet of Things J.* , vol. 6, no. 3, pp. 5324-5335, Jun. 2019.

[18] R. Talak and E. Modiano, “Age-delay tradeoffs in queueing systems,” *IEEE Trans. Inf. Theory*, vol. 67, no. 3, pp. 1743-1758, Mar. 2021.

[19] L. Hu, Z. Chen, Y. Dong, Y. Jia, L. Liang and M. Wang, “Status Update in IoT Networks: Age-of-Information Violation Probability and Optimal Update Rate,” *IEEE Internet Things J.*, vol. 8, no. 14, pp. 11329-11344, Jul. 2021.

[20] R. Wang, Y. Gu, H. Chen, Y. Li, and B. Vucetic, “On the age of information of short-packet communications with packet management,” in *Proc. IEEE Global Commun. Conf. (GLOBECOM)*, Waikoloa, HI, USA, Dec 2019, pp. 1–6.

[21] B. Yu, Y. Cai, D. Wu and Z. Xiang, “Average age of information in short-packet-based machine type communication,” *IEEE Trans. Veh. Technol.*, vol. 69, no. 9, pp. 10306-10319, Sep. 2020.

[22] B. Han, Y. Zhu, Z. Jiang, Y. Hu, and H. D. Schotten, “Optimal blocklength allocation towards reduced age of information in wireless sensor networks,” in *Proc. IEEE Global Commun. Conf. (GLOBECOM) Wkshps.*, Waikoloa, HI, USA, Dec. 2019, pp. 1–6.

[23] J. Cao, X. Zhu, Y. Jiang and Z. Wei, “Can AoI and delay be minimized simultaneously with short-packet transmission?” in *Proc. IEEE Conf. Comput. Commun. (INFOCOM) Workshops*, Vancouver, BC, Canada, 2021, pp. 1-6.

[24] J. Cao, X. Zhu, Y. Jiang, Z. Wei and S. Sun, “Information age-delay correlation and optimization with finite block length,” *IEEE Trans. Commun.*, vol. 69, no. 11, pp. 7236-7250, Nov. 2021.

[25] R. Devassy, G. Durisi, G. C. Ferrante, O. Simeone and E. Uysal, “Reliable transmission of short packets through queues and noisy channels under latency and peak-age violation guarantees,” *IEEE J. Sel. Areas Commun.*, vol. 37, no. 4, pp. 721-734, Apr. 2019.

[26] C. Liu and M. Bennis, “Taming the tail of maximal information age in wireless industrial networks,” *IEEE Commun. Lett.*, vol. 23, no. 12, pp. 2442-2446, Dec. 2019.

[27] M. K. Abdel-Aziz, S. Samarakoon, C. Liu, M. Bennis and W. Saad, “Optimized age of information tail for ultra-reliable low-latency communications in vehicular networks,” *IEEE Trans. Commun.*, vol. 68, no. 3, pp. 1911-1924, Mar. 2020.

[28] M. Klügel, M. H. Mamduhi, S. Hirche and W. Kellerer, “AoI-penalty minimization for networked control systems with packet loss,” in *Proc. IEEE Conf. Comput. Commun. (INFOCOM) Workshops*, Paris, France, May 2019, pp. 189-196.

[29] J. P. Champati, M. H. Mamduhi, K. H. Johansson and J. Gross, “Performance characterization using AoI in a single-loop networked control system,” in *proc. IEEE Conf. Comput. Commun. (INFOCOM) Workshops*, Paris, France, May 2019, pp. 197-203.

[30] C. -H. Tsai and C. -C. Wang, “Unifying AoI minimization and remote estimation — optimal sensor/controller coordination with random two-way delay,” in *Proc. IEEE Conf. Comput. Commun. (INFOCOM)*, Virtual, Jul. 2020, pp. 466-475.

[31] A. M. Girgis, J. Park, M. Bennis and M. Debbah, “Predictive control and communication co-design via two-way gaussian process regression and AoI-aware scheduling,” *IEEE Trans. Commun.*, vol. 69, no. 10, pp. 7077-7093, Oct. 2021.

[32] K. Huang, W. Liu, M. Shirvanimoghaddam, Y. Li and B. Vucetic, “Real-time remote estimation with hybrid ARQ in wireless networked control,” *IEEE Trans. Commun.*, vol. 19, no. 5, pp. 3490-3504, May 2020.

[33] E. Fountoulakis, N. Pappas, M. Codreanu and A. Ephremides, “Optimal sampling cost in wireless networks with age of information constraints,” in *Proc. IEEE Conf. Comput. Commun. (INFOCOM) Workshops*, Toronto, ON, Canada, 2020, pp. 918-923.

[34] S. Roth, A. Arafa, A. Sezgin and H. Vincent Poor, “Short Blocklength Process Monitoring and Scheduling: Resolution and Data Freshness,” *IEEE Trans. Wirel. Commun.*, Early Access 2021.

[35] X. Wang, C. Chen, J. He, S. Zhu and X. Guan, “AoI-aware control and communication co-design for industrial IoT systems,” *IEEE Internet of Things J.*, vol. 8, no. 10, pp. 8464-8473, May, 2021.

[36] P. M. de Sant Ana, N. Marchenko, P. Popovski and B. Soret, “Age of loop for wireless networked control systems optimization,” in *Proc. IEEE Annual International Symposium on Personal, Indoor and Mobile Radio Communications*, Helsinki, Finland, 2021, pp. 1-7.

[37] D. P. Bertsekas and R. G. Gallager, *Data networks*. Prentice Hall, 2ed., 1992.

[38] A. Lancho, J. Östman, G. Durisi, T. Koch and G. Vazquez-Vilar, “Saddlepoint approximations for short-packet wireless communications,” *IEEE Trans. Wirel. Commun.*, vol. 19, no. 7, pp. 4831-4846, Jul. 2020.

[39] M. Shirvanimoghaddam *et al.*, “Short block-length codes for ultra-reliable low latency communications,” *IEEE Commun. Mag.*, vol. 57, no. 2, pp. 130–137, Feb. 2019.

[40] C. She, C. Yang and T. Q. S. Quek, “Joint uplink and downlink resource configuration for ultra-reliable and low-latency communications,” *IEEE Trans. Commun.*, vol. 66, no. 5, pp. 2266-2280, May 2018.

[41] P. Park, J. Araújo and K. H. Johansson, “Wireless networked control system co-design,” in *Proc. IEEE Int. Conf. Network. Sens. Control*, Delft, Netherlands, Apr. 2011, pp. 486-491.

[42] J. P. Hespanha, P. Naghshtabrizi and Y. Xu, “A survey of recent results in networked control systems,” *Proc. of the IEEE*, vol. 95, no. 1, pp. 138-162, Jan. 2007.

[43] B. Han, S. Yuan, Z. Jiang, Y. Zhu and H. D. Schotten, “Robustness Analysis of Networked Control Systems with Aging Status,” in *Proc. IEEE Conf. Comput. Commun. (INFOCOM)*, virtual, Jul. 2020, pp. 1360-1361.